



universität
wien

DIPLOMARBEIT

Rhizobial symbiosis related response of *Medicago truncatula* to salt and drought stress

Verfasser:

Reinhard Josef Turetschek

angestrebter akademischer Grad

Magister der Naturwissenschaften (Mag.rer.nat.)

Wien, 2013

Studienkennzahl lt. Studienblatt: A 190 445 456

Studienrichtung lt. Studienblatt: Lehramtstudium, Biologie und Umweltkunde,
Geographie und Wirtschaftskunde

Betreuerin: Dipl. Biol. Dr. rer. nat. Stefanie Wienkoop

Contents

1. Introduction	1
1.1. <i>Medicago truncatula</i> as model organism.....	1
1.2. Proteomic approach	2
1.3. General objectives.....	3
2. Material and methods	4
2.1. Cultivation and experimental settings.....	4
2.2. Physiological parameters	5
2.2.1 Stomatal conductance	5
2.2.2 Specific leaf area (SLA)	6
2.2.3 Osmotic potential (Ψ_s) of leaf solution	6
2.2.4 Leaf water potential (Ψ_T).....	7
2.2.5 Water content (WC).....	7
2.2.6 Electrical conductance	7
2.3. Protein extraction	8
2.3.1 Shoot protein extraction.....	8
2.3.2 Root protein extraction	8
2.4. Protein digestion	8
2.5. Nano ESI LC-MS/MS.....	9
2.6. Data mining.....	9
2.6.1 Database dependent approach	9
2.6.2 Functional categorisation of significant changing proteins.....	10
2.6.3 Mass accuracy precursor alignment (MAPA) approach.....	10
2.6.4 Statistical analysis.....	10

3. Results.....	10
3.1. Physiological characterization of salt and drought stress	11
3.2. Analysis of identified proteins	13
3.2.1 Normalization of different MS-methods	19
3.2.2 Root salt stress responsive proteome (see A.3)	20
3.2.3 Shoot salt stress responsive proteome (see A.4 - A.5)	21
4. Discussion	23
4.1. Stress determination and physiological response	23
4.2. Complicated data mining of different MS-methods	25
4.3. Proteome stress modifications depending on nutritional phenotypes	25
4.3.1 Shoot proteome.....	25
4.3.2 Root proteome	27
5. Summary	31
6. Zusammenfassung	32
7. Bibliography.....	33
8. Acknowledgement.....	40
A. Attachments	I
A.1. Supplemental nutrient solutions EC-values	I
A.2. Formulations.....	I
A.3. Significant changing root proteins	II
A.4. Significant changing shoot proteins	VIII
A.5. Significant changing shoot peptides.....	X
A.6. Curriculum vitae.....	XI

List of figures

Figure 2.1: Workflow	4
Figure 2.2: Experimental setup	5
Figure 3.1: Leaf water potential and stomatal conductance	13
Figure 3.2: Functional distribution of 1521 proteins.....	15
Figure 3.3: PCA-plot of proteomic data.....	16
Figure 3.4: Overlap of altering proteins during salt stress for root and shoot.....	18
Figure 3.5: Proteins with similar control levels or stress levels.....	19
Figure 3.6: MS2 and full scans of different datasets.....	20

List of tables

Table 3.1: Physiological parameters of N-fed and N-fix plants.....	11
Table 3.2: Protein up- and down-regulation of N-fed and N-fix plants.....	18
Table 8.1: Electrical conductivity of nutrient solutions	I
Table 8.2: TY-medium <i>S. meliloti</i>	I
Table 8.3: Cultivation medium <i>S. meliloti</i>	I
Table 8.4: Salt stress responding root proteins	II
Table 8.5: Salt stress responding shoot proteins	VIII
Table 8.6: Salt stress responding shoot peptides.....	X

List of abbreviations

ϵ_m	osmolality
g_s	stomatal conductance
Ψ_s	osmotic potential
Ψ_T	water potential
Aa	amino acid
AlaAT	alanine aminotransferase
BLAST	basic local alignment search tool
CA	calibration area
CV	coefficient of variance
DW	dry weight
EC	electrical conductance
E-value	expect-value
FDR	false discovery rate
FW	fresh weight
GCS	glycine decarboxylase complex
GTP	guanosine triphosphate
LA	leaf area
LC	liquid chromatography
LWC	leaf water content
MAPA	mass accuracy precursor alignment
MS	mass spectrometry
PC	pixels calibration
PCA	principal component analysis
PF	pixels foliage
PIP	plasma membrane intrinsic protein
PP	polypropylene
PPFD	photosynthetic photon flux density
ProMEX	protein mass spectra extraction
PTM	posttranslational modifications
ROS	reactive oxygen species
SC	spectral count
SLA	specific leaf area
SWC	soil water content
TCA cycle	tricarboxylic acid cycle

1. Introduction

1.1. *Medicago truncatula* as model organism

Although being surrounded by nitrogen this element is one of the limiting constraints in plant growth. Adaptations to nutrient-poor environments include symbiotic associations with bacteria. Those are phylogenetically widespread indicating an early evolution. The development of nitrogen-fixing symbiosis likely happened simultaneously with the evolution of arbuscular mycorrhiza, a symbiosis with phosphate acquiring fungi (Markmann et al. 2008). The two major forms occurring for nitrogen-fixation are actinorhiza, mainly appearing in trees, and rhizobia. Both form so called root nodules, specialized organs allocating bacteria which are capable of converting atmospheric nitrogen into ammonia. Legumes – intensively examined for rhizobia interaction - evolved approximately 60 million years ago (Ojciechowski et al. 2004) and are one of the most diverse families of angiosperms with 745 genera consisting of 19500 species (Stevens 2001). With 41 domesticated crop species legumes are the most important agricultural plants after Poaceae (Harlan, 1992). As root-nodule generating plants legumes enhance the quality of subsequent crops as they maintain soil fertility and therefore reduce the need for chemical fertilizers. Moreover, seeds contain large quantities of nitrogen in the form of proteins making them essential for a balanced vegetarian diet (Wyk 2005).

For detailed investigation on a molecular level plant model organisms were determined in the past decades. In the 1940s *Arabidopsis thaliana* was already examined on mutations and was fully sequenced in 2000 (Arabidopsis Initiative). Today it is a widely used model organism for studies in different biological areas (Platt et al., 2010; Coelho et al. 2007). Because of their symbiosis with bacteria and their economic importance legumes required further research and therefore a representative model. Although the most common legumes are beans and peas they do not fulfil the requirements of a model organism. In the late 1990s *Lotus japonica* and *Medicago truncatula* established as model plants (Cook 1999). *Medicago truncatula* is closely related to alfalfa and *Pisum sativum*, which are important forage cultivars. It has a relatively small diploid genome ($n=8$) of ~500 Mbp compared to *Pisum sativum* with ~5000 Mbp, a rapid generation time (2-3 months) and is self fertile (Sato et al. 2010, Bell et al. 2001). Furthermore, its high seed productivity, susceptibility to genetic transformation and high phenotypic plasticity make it suitable for research (Trieu et al. 2000). Its genome is now to ~94% sequenced (Young et al. 2011) counting 268712 expressed sequence tags on the DFCI Medicago Gene Index (release 11.0).

This facilitates functional annotation of protein sequences, not only for the host plant but also for its bacterial symbiont.

1.2. Proteomic approach

Technological progress in genome sequencing made tremendous leaps during the past decade. With Next Generation Sequencing the throughput enormously increased and reagent costs substantially lowered (Weckwerth 2011). The assembling of sequences and analysis for homology with sequences in public databases using BLAST algorithms allowed the translation into peptides and the annotation of their biological function (Cantacessi et al. 2010).

Even though the number of genes is clearly related to the number of proteins it is not the case that all proteins predicted in an organism can also be found. Several reasons do not allow us to detect all proteins predicted. First, the actual protein composition is subjected to many external factors like the developmental stage, stress and other conditions an organism is exposed to. Moreover during the expression of a protein there are possible modifications that are not encoded in the sequence of its gene. Messenger RNAs for example can be spliced and form a different final mRNA string. Variability within the proteome expands even further as most proteins show some form of posttranslational modifications (PTM) like phosphorylation, acylation or glycosylation. These modifications affect activity, subcellular localization, stability, and interaction with other proteins or molecules (Seo & Lee 2004).

This work focuses on the whole proteome which is defined by all proteins expressed in a given organism (*M. truncatula*) under defined circumstances. As an overview of all proteins expressed at a specific point of time shall be given, this work follows a bottom-up approach in which peptide masses of digested proteins including their PTMs are measured via MS (mass spectrometry) and then compared to sequences in databases generated from genomic and transcriptomic information. In past decades mass spectrometry came to be more efficient and accurate thus now being a common tool used in proteomics. Since analysis with MS only works in the gas phase it was a major problem to gently evaporate large molecules. The invention of MALDI (Matrix Assisted Laser Desorption Ionization) and ESI (Electro Spray Ionization) enabled measurements of proteins and are commonly coupled to pre-fractionation techniques like LC (liquid chromatography) in combination with tandem MS where full scan spectra are performed in order to analyse the parent ion. This usually happens in form of collision induced dissociation (CID). As most fragments are single charged, those likely have a larger m/z than a double charged parent ion.

This method results in an output of spectral counts per peptide allowing a relative quantification of detected proteins (Wienkoop et al. 2006).

1.3. General objectives

With the control over plant growth and the onset of agriculture humans were able to become sedentary in many parts of the world. In the past millennia breeding of plants was essential for the rise of human civilization. Especially in the 19th century the discoveries of Gregor Mendel on *Pisum sativum* fundamentally contributed to the knowledge of breeding and subsequently to the field of genetics. First, breeders mainly aimed to maximize crops by seed size and quantity. Other criteria were then the quality of food like the content of proteins and taste. And certainly the control over pest infestation always played a major role in breeding from the beginning on. But not only biotic stress as field pest was considered when farming new kinds of seeds. As for growing at higher latitudes special varieties were demanded which are more adapted to a shorter photoperiod, lower temperature, less light intensity as well as a shorter growing season. Abiotic stress resistance becomes more important as humans are now facing self made problems which include further growth of human population, elevating NO₂ levels and a rapid proceeding climate change. The latter involves increasing CO₂ levels causing rise of average temperature. Hence breeding of better adapted cultivars is the recent challenge which must be accepted by using the most appropriate means available. Many authors (Gálvez et al., 2005, Del Castillo et al., 1994, Almeida et al. 2000) so far dealt with different stress concerning the most important crop plants. One of the main factors limiting plant growth is drought stress (Smirnoff 1998). In the upcoming century rising temperatures are one of our main concerns, which include increased drought and subsequently salt stress. Due to their special relationship with bacteria, legumes behave very different when exposed to drought stress and were therefore already examined (Staudinger 2010, Estíbaliz Larrainzar et al. 2007, Larrainzar et al. 2009). As symbiosis with rhizobial bacteria mainly depends on the nitrogen available in the soil and not that much attention was yet given to elevated salinity, in this work I will

(1) assess the physiological status of *M. truncatula* exposed to salt and drought stress under different nitrogen constraints.

In the past decade proteomics turned out to become a powerful tool for breeding as well as for the understanding of biological systems. Hence I will accomplish the

(2) detection and relative quantification of the protein level of salt stressed plants

(3) in order to determine varying proteins between different treatments.

2. Material and methods

An overview of the workflow is depicted in fig. 2.1. It comprises of the assessment of the physiological status and the identification of the proteome via shotgun LC MS/MS.

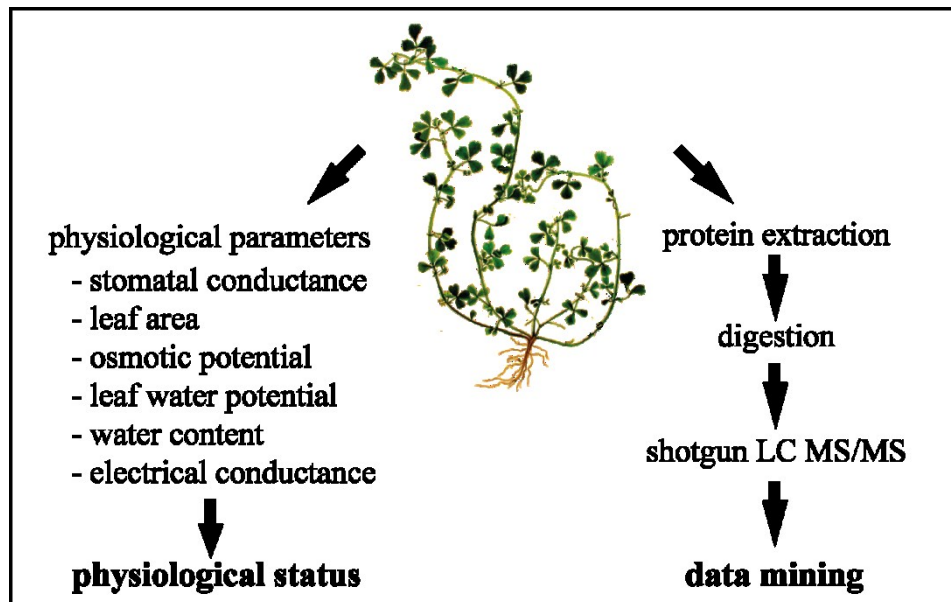


Figure 2.1: The workflow includes the assessment of the physiological status as well as the identification and quantification of proteins

2.1. Cultivation and experimental settings

The experiment was setup according to Larrainzar et al. (2007) with *M. truncatula* ‘Jemalong A17’ plants. Seeds were scarified in sulphuric acid for maximum 7 min, sterilized with 5% sodium hypochlorite for 3 min and rinsed with water. The seeds were then placed on 0.8% agar-plates and stored 1 d in darkness at 4°C, 3 d at room temperature and 1 d at light. Seedlings were then piqued into 800 ml PP pots with vermiculite:perlite substrate (5:2, v/v) and grown in a climatic chamber under controlled environmental conditions: 14 h photoperiod/10 h darkness, 750 $\mu\text{mol m}^{-2}\text{s}^{-1}$ PPFD, 22°C/16°C day/night temperature, 60-70% relative humidity. Fig. 2.1 shows the experimental process. During the first week the seedlings were watered with a nutrient solution (Evans HJ, 1981) containing 0.5 mM NH_4NO_3 . The second week seedlings received concentrations of 2.5 mM NH_4NO_3 . After 15 d the plants were randomly split in two sets: Nitrogen fertilized and inoculated plants. Inoculation was carried out on day 15 and 17 by adding 1 ml bacterial solution (*Sinorhizobium meliloti*) to each pot. *S. meliloti* was cultivated and stored according to Staudinger (2010) on TY-0,8 % agar medium (see A.1).

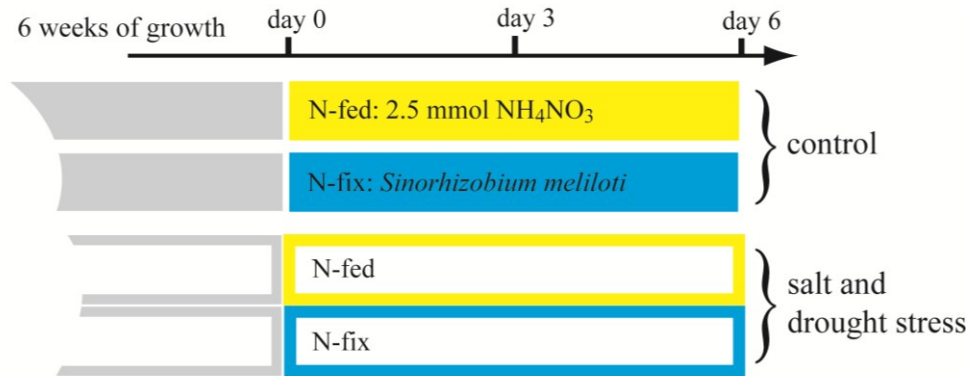


Figure 2.2: Experimental setup and days of record: Fertilized plants (N-fed) are indicated yellow, inoculated plants (N-fix) are indicated blue

Two days before inoculation a bacterial solution (see A.1.) was prepared for growth of *S. meliloti* in an incubator (innova44, New Brunswick Scientific, USA). From day 22 on the inoculated plants were watered with nitrogen-free nutrient solution in order to enable root nodulation. The nitrogen fertilized set received nutrient solution containing 2.5 mM NH_4NO_3 . After 42 d of growth a subset of N-fertilized and inoculated plants was exposed to either salt or drought stress for a duration of 6 d (shown in fig. 2.2). The remaining plants were kept as control. Salt stressed plants were watered with 200 mM sodium chloride nutrient solution to field capacity. Drought stressed plants did not receive any nutrient solution.

2.2. Physiological parameters

Physiological measurements and sampling were carried out 1 d before (referred to as “day 0”), 3 d and 6 d after the onset of stress to obtain mild and moderate stressed plants. All assessed parameters are listed and described below. Measurements of leaf area, water potential, dry matter content and electrical conductance were made on the same samples.

2.2.1 Stomatal conductance

Stomatal conductance g_s was measured on fully expanded terminal leaves 2-3 h after the onset of the light period. Seven records were taken with a steady state (PMR-4, PP Systems, Hitchin, UK) and a dynamic porometer (AP4, Delta-T Devices Ltd, UK) with a measurement surface of 28 and 56 mm² respectively. Two measurement devices were used because of defects. The inlet airflow of the steady state porometer was kept constant on 75 ml/min. PPFD, air temperature, and air humidity of the inlet and outlet airflow were measured by the steady state porometer in order to calculate g_s . The dynamic porometer in contrary measures the time duration it takes to raise humidity from a specific value for calculation of g_s . Records were taken when values remained stable after ~10-20 s.

2.2.2 Specific leaf area (SLA)

Leaf area was determined corresponding to O'Neal, Landis, & Isaacs (2002) by using a desktop scanner (CanoScan LiDE 90, Canon). Leaves of control and stressed plants were cut off with a petiole length of ~1 cm and spread out on the scanner together with three calibration areas of 1, 2 and 3 cm² respectively. To obtain a high resolution image, color scans were made at 400 dpi and saved in jpeg format (Adobe Photoshop CS3). For pixel quantification a black and white picture was created by applying a color threshold of 175 (GIMP 2.6.11.). By using the cutting tool and the histogram function the pixels of the leaf and calibration area were displayed. The leaf area was calculated as follows:

$$LA = \frac{CA * PF}{PC}$$

where LA stands for leaf area, CA is calibration area, P is the number of pixels of the foliage (PF) and calibration area (PC) pixels. Further, specific leaf area (SLA) was calculated by following equation:

$$SLA = \frac{LA}{DW}$$

where DW stands for dry weight of the leaves.

2.2.3 Osmotic potential (Ψ_s) of leaf solution

Fully expanded leaves were cut off quickly and moved into precooled 50 ml Eppendorf-tubes which were immediately put into liquid nitrogen. The frozen leaves were crushed, transferred in 24 ml syringes and heated up for 10 s in a microwave (M760, Philips). The defrosted leaves were squeezed out into 1.5 ml Eppendorf-tubes and put on ice for measurement. Two records were taken of each sample with a freezing point osmometer (3MO plus, Advanced Instruments, Inc.). The osmolality is determined by the measurement of the depression of freezing point ΔT as follows

$$\varepsilon_m = \frac{\Delta T}{1.86} * 1000 \text{ mosm/kg}$$

Further, osmotic potential was calculated with the van't Hoff equation.

$$\Psi_s = -RT_{25} * c_s$$

where RT_{25} is the gas constant at 25°C and c_s is the leaf sap osmolality.

2.2.4 Leaf water potential (Ψ_T)

Measurements were carried out according to Scholander (1965). The water potential was measured on leaves at 2-3 h after onset of the photoperiod with a petiole length of ~3-4 cm (3005 – Original Plant Water Status, Soilmoisture Equipment Corp.). Chamber pressure was increased with a speed of ~0.3 MPa/s.

2.2.5 Water content (WC)

After measuring stomatal conductance and water potential leaves were cut off with a petiole length of ~1 cm. Shoots were cut off at substrate level and roots were freed of substrate. Leaves, shoot and root were weighed separately, put into paper envelopes and dried at 80°C for 3 d. Substrate was dried in 2 l glasses at 100°C for 4 d. Water content was calculated as follows

$$WC = \frac{FW - DW}{FW}$$

where FW refers to fresh, DW to dry weight. Soil water content was determined according to Gardner et al (2000) by following formula

$$SWC = \frac{FW - DW}{DW}$$

where SWC is the soil water content. The water content of the soil is the mass of water per unit mass of dry soil.

2.2.6 Electrical conductance

Saturation for 75 g dry substrate was determined at 50 g water. According to Corwin & Lesch (2005) the saturated substrate was shook in proportion of 1:1 with water for 1.5 h in an incubator (innova44, New Brunswick Scientific, USA). The solution of one sample was filtrated to two technical replicates and subsequently measured (Orion 4-Star Plus pH/Conductivity Meter,

Thermo Scientific Fisher, Wien). Three biological replicates of dried leaves were dissolved in deionized water (1:3, w/w) for 5 min to determine electrical conductivity.

2.3. Protein extraction

Samples for protein extraction are from salt stressed plants as described in chapter 2.1. Three biological replicates of each condition were harvested 2 h after onset of the light period and immediately quenched in liquid nitrogen. Shoot and root material was ground with pestle and mortar under constant addition of liquid nitrogen. Until grinding samples were stored at -80°C for lyophilisation (Alpha 2-4, Martin Christ, 4 Pa, -18°C, 1-2 d). After lyophilisation the material was stored at -20°C until extraction.

2.3.1 Shoot protein extraction

50 mg dry leaves were homogenized in 1.5 ml urea buffer (50 mM hepes, 8 M urea, ph 7.8) and centrifuged (10000 g, 10 min, 4°C). The urea soluble proteins in the supernatant were transferred and precipitated for 14-16 h at -20°C in 5 volumes of precooled (-20°C) acetone containing 0.5% β -mercaptoethanol. After centrifugation (4000g, 4°C, 15 min) the protein-pellet was washed in 2 ml methanol (-20°C), centrifuged (4000g, 4°C, 10 min) and air-dried.

2.3.2 Root protein extraction

Extraction of root proteins was performed according to (Carpentier et al. 2005). 50 mg dry roots were homogenized in 1.5 ml ice-cold extraction buffer (50 mM TrisHCL ph 7.5, 5 mM EDTA, 0.7 mM sucrose, 1% PVPP (w/v), 1 mM PMSF, 5 mM DTT) and after adding 1.5 ml phenol (Roti-Phenol, ph 7.5-8, Roth) for further homogenization, shook for 30 min at 4°C. After centrifugation (4000 g, 30 min, 4°C) the upper phenolic phase was transferred and precipitated in 7 ml precooled (-20°C) acetone for 14-16 h. The centrifuged pellet (4000 g, 15 min) was then air dried for further processing.

2.4. Protein digestion

Air-dried pellets were dissolved in 800 μ l urea buffer. Protein concentration was determined by a Coomassie blue colorimetric method (Bradford 1976) using BSA as standard. 100 μ g proteins were first digested in urea buffer for 5 h at 30°C with endopeptidase Lys-C (1:100 v/v, Roche, Mannheim, Germany). For the second digestion step a trypsin buffer (10% ACN, 50 mM Am-Bic, 2 mM CaCl_2) was added to obtain a final urea concentration of 2 M. After digestion (12 - 14 h, 37°C) with poroszyme immobilized trypsin beads (1:10, v/v, Applied Biosystems, Darmstadt,

Germany) the digests were desalted with C18-SPEC 96-well plates (Varian, Darmstadt, Germany) according to manufacturer's manual. The peptides were eluted with methanol, split to two technical replicates and vacuum dried.

2.5. Nano ESI LC-MS/MS

Vacuum dried peptides were dissolved in 5% acetonitrile and 0.1% formic acid resulting in a final concentration of 0.1 µg proteins in 1 µl solution. 0.5 µg proteins of each sample were randomly loaded on a monolithic column (15 cm length, 50 µm internal diameter Merck, Darmstadt, Germany) via an autosampler (HTC PAL, CTC Analytics) and separated during a 120 min (leaves) and 85 min (root) gradient from 80% solvent A (0.1% formic acid) to 90% of solvent B (80% acetonitrile). Mass spectral analysis was performed on an LTQ Orbitrap (Thermo Scientific Fisher) in an acquisition cycle of 9 scan events: a full range scan (Orbitrap) with a scan-range from 350 to 1800 m/z and 8 MS2 scans (linear ion trap) of the most abundant m/z in the full range scan. Half of the leaf replicates were measured with 5 MS2-scans and a scan range from 300 to 1800 m/z. For all samples, an exclusion mass list of 500 was set to an exclusion time of 60 s and a width of 10 ppm, repeat count was set to 1 with a duration of 20 s. Minimum signal threshold counts was set to 1000. Charge state screening was enabled with rejection of unsigned and +1 charge states.

2.6. Data mining

2.6.1 Database dependent approach

For mass spectral analysis the SEQUEST search-algorithm (Eng et al. 1994) combined with Proteome Discoverer (v 1.3, Thermo Fisher Scientific Inc.) was used to search MS data against a fasta file which was created from a *Medicago spp.* and *Sinorhizobium spp.* subset of UniProt-Knowledgebase (<http://www.uniprot.org/>) containing 63688 sequences in April 2012. *In silico* peptide lists were compiled with trypsin as digestion enzyme, a maximum of 3 missed cleavages, methionine oxidation and acetylation as dynamic modification. Tolerance for mass was set to 10 ppm for precursor ions and 0.8 Da for fragment ions. To exclude fake matches the quality of protein identifications was assessed by a search against a decoy database containing reverse sequences. Only peptides with a FDR of high confidence ($\leq 0.01\%$) identification and a minimum Xcorr of 2.2 as well as proteins with at least two different peptides were considered valid. All peptide spectra evaluated are stored in the *PromEX* database (Wienkoop, 2012) which can be accessed online (www.promexdb.org).

2.6.2 Functional categorisation of significant changing proteins

Functional categorisation of all significant changing putative proteins, which are so far uncharacterized and unknown in function, was carried out via BLAST. Main parameters for categorisation were sequence similarities of the proteins derived from other phylogenetically related organisms. Sequence similarity and E-value are provided in tab. A.3-A.4.

2.6.3 Mass accuracy precursor alignment (MAPA) approach

Leaf data was additionally analyzed by the ProtMAX software (<http://promex.pph.univie.ac.at>) described by Hoehenwarter et al. (2008). Data conversion of .raw to .mzXML files was performed with the program *MM File Conversion* (Cleveland, OH, USA, <http://www.massmatrix.net/mmcgi/downloads.py>). A target list, containing retention time (RT) and m/z values of the peptides, was obtained by the previous database dependent approach and used as search filter to analyse peptide abundance in precursor scans. Spectra within the retention time of 20-110 min and a deviation of ± 1 min from the target list scans were regarded. Intensity threshold was set to 20%. Ion intensities of demanded m/z values were used for further process.

2.6.4 Statistical analysis

Physiological data was analysed by comparing controls with either salt or drought stressed phenotypes. A student's T test was performed with significant differences at $p < 0.05$. For statistical analysis of MS data a protein must at least be detected in four out of the six replicates in one condition to be valid for all treatments. Proteins with less SC are not regarded for further analysis. If a protein was detected in 4 or 5 out of 6 replicates, the missing values were filled with the K-nearest neighbor method. If the protein was detected in 3 or less replicates, missing values were filled with the lowest value of SC of this protein from all samples and was multiplied by 0.5 and again multiplied by a random value between 0 and 1. Applying this method ensures a more precise calculation of the magnitude of changing and significant values between control and stressed plants due to filling of completely missing SC values in a full condition.

3. Results

As legumes are one of the most important crop plants world wide (Harlan 1992) we were interested in the early stress response to drought- and salt-stress. Metabolomic and proteomic research already proved the effect of nitrogen-fixing bacteria on *Medicago truncatula* under drought stress (Larrainzar et al. 2009) but still leaving open questions demanding further

research. Accordingly, first I assessed the differential physiological response to drought and salt stress and second, to gain further insight in the proteomic response to salt stress, I focused on the different protein levels in roots and shoots.

3.1. Physiological characterization of salt and drought stress

Physiological parameters were recorded to pinpoint the degree of stress. Thus, concerning drought stress, the most appropriate parameter indicating stress is the relative water content of different organs as well as of the substrate. To estimate the level of photosynthesis, stomatal conductance was used as parameter. Osmolality and water potential were measured to gain further insights to the plants water balance. All records were taken at day 6 of drought or salt stress. Significant values are summarized in table 3.1.

Table 3.1: Physiological parameters of N-fed (a) and N-fix (b) plants; values represent mean and standard deviation; letters a,b,c indicate significant changes ($p < 0.05$). Not applied methods are shown as “n.a.”. Asterisk indicate significant differences between nutritional phenotypes.

(a) N-fed

Parameter	Control	Drought	Salt
DW	6.287±1.316 a*	4.857±2.138 a	10.013±2.275 a
LWC	0.838±0.006 a	0.795±0.011 b	0.843±0.002 a
SWC	4.277±0.046 a	1.53±0.233 b	3.891±0.11 a
Ψ_s leaf (MPa)	-0.961±0.012 a	n.a.	-1.554±0.165 b
Ψ_T (MPa)	-0.708±0.007 a	-0.908±0.080 b	-0.685±0.194 a
g_s (mmol H ₂ O m ⁻² s ⁻¹)	413±154 a	57±15 b	40±12 b
EC leaf (μS/cm)	1391±60 a	n.a.	1991±261 b
EC substrate (μS/cm)	3146±164 a	n.a.	11073±797 b
SLA (cm ² /g)	311±4.67 a*	253±21.41 b	300±8.3 a

(b) N-fix

Parameter	Control	Drought	Salt
DW	1.922±0.380 a*	3.54±0.61 b	2.142±0.740 a
LWC	0.895±0.031 a	0.88±0.01 a	0.904±0.016 a
SWC	3.903±0.228 a	1.889±0.192 b	3.861±0.274 a
Ψ _s leaf (MPa)	-1.084±0.041 a	n.a.	-1.412±0.127 b
Ψ _T leaf (MPa)	-0.75±0.1 a	-1.158±0.102 b	-0.734±0.348 a
g _s (mmol H ₂ O m ⁻² s ⁻¹)	437±130 a	83±16 b	39±15 c
EC leaf (μS/cm)	1307±118 a	n.a.	2301±209 b
EC substrate (μS/cm)	2764±192 a	n.a.	11982±777 b
SLA (cm ² /g)	237±4.68 a*	252.17±4.9 a	250±10.56 a

Concerning *leaf water content* (LWC) only the actual water content of the leaf was determined with no regard to the relative water content. Generally symbiotic plants do show higher LWC compared to N-fed plants. During drought stress the LWC of N-fed plants decreased significantly by 5.2%, whereas the LWC of symbiotic plants almost remained at initial levels. It is noticeable that the LWC of salt stressed plants also remained close at control levels.

Substrate water content (SWC) was difficult to assess as the received amount of nutrient solution differed slightly between plants. However, all plants were irrigated 2 h before records were taken in order to guarantee field capacity at the time of measurement. Drought exposed plants show a significant decrease in SWC, whereas symbiotic plants show less water loss (51.6%) in the substrate than fertilized ones (64.4%). For salt exposed plants there is no significant loss of water in the substrate compared to the control plants.

The *osmotic potential* (Ψ_s) was only measured on control and salt stressed plants. Calculation was carried out through osmolality records and the van't Hoff equation. Both treatments, fertilized and symbiotic plants show a significant decrease in Ψ_s during elevated salinity. The data shows that there is a significant decrease in fertilized plants (61.7%) as well as in symbiotic plants (30.3%). Although N-fed plants do show a higher decrease in the osmotic potential, there is no significant difference compared to symbiotic plants.

Leaf water potential (Ψ_T) was determined with the scholander bomb and carried out for all conditions. As shown in fig. 3.1, a significant decrease for N-fix (54.4%) but not N-fed (28.2%) phenotypes during drought is present. Water potential in salt stressed plants remained at approximately the same level as in control plants (-0.69 to -0.75 MPa).

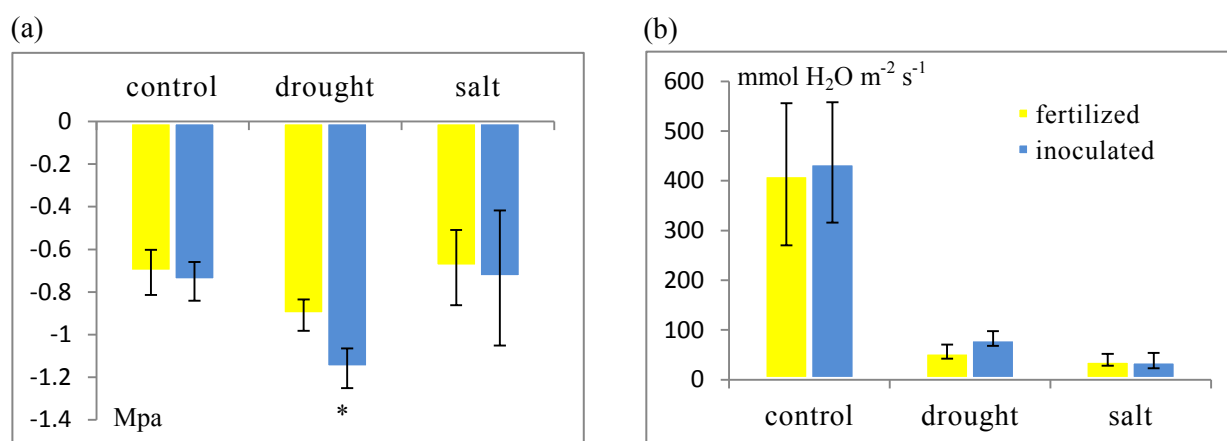


Figure 3.1: (a) Leaf water potential (Ψ_T) and (b) stomatal conductance (g_s), asterisk indicate significant differences (p-value<0.05)

For *stomatal conductance* (g_s), fertilized and symbiotic plants are approximately at the same level with 413 and 437 $\text{mmol H}_2\text{O m}^{-2} \text{s}^{-1}$ respectively. Both treatments respond similar to water deprivation as g_s significantly declined in N-fed (86.2%) and N-fix (81%) drought stressed plants as shown in figure 3.1. Stomatal reaction to salt stress was slightly more intense compared to drought stress. Fertilized plants show a decrease of 90.3%, whereat symbiotic plants show a decrease of 91.1%.

Electrical conductivity shows significant differences in leaf, stem and substrate extracts of salt stressed plants. Stem extracts are not listed in table 3.1 as those are very similar to leaves. No differences could be determined between N-fix and N-fed plants. Supplemental, a table of the nutrient solutions EC is provided in the attachments section (A.1)

Assessment of the *specific leaf area* revealed only a significant decrease in fertilized plants during drought but not symbiotic ones. Furthermore, N-fed phenotypes generally show higher SLA than N-fix phenotypes.

3.2. Analysis of identified proteins

The measurement of purified root and shoot proteins of day 0, 3 and 6 of all treatments resulted in 186370 recorded spectra and the identification of 1521 proteins which were functionally categorized and visualized (fig.3.2) with mapman (Thimm et al. 2004, Staudinger et al. 2012). Of all proteins found, 1093 were detected in both, N-fed and N-fix plants, 190 proteins were only found in N-fed plants and 238 proteins could exclusively be determined in N-fix plants. Fig. 3.2 displays all proteins categorised in root (434 - indicated blue) or leaf (618 - indicated green) determined proteins and proteins found in all parts of the plants (469 - indicated white). Functional categorisation of all proteins reveals protein regulation as dominant group (26%), whereat 56% proteins of this category belong to protein synthesis and 25% to protein

degradation. Proteins belonging to the photosystem make up 10% followed by endosymbiotic proteins of *Sinhorizobium meliloti* (8%) and amino acid metabolism (5%). Proteins listed by their functional category can be found in figure 3.2.

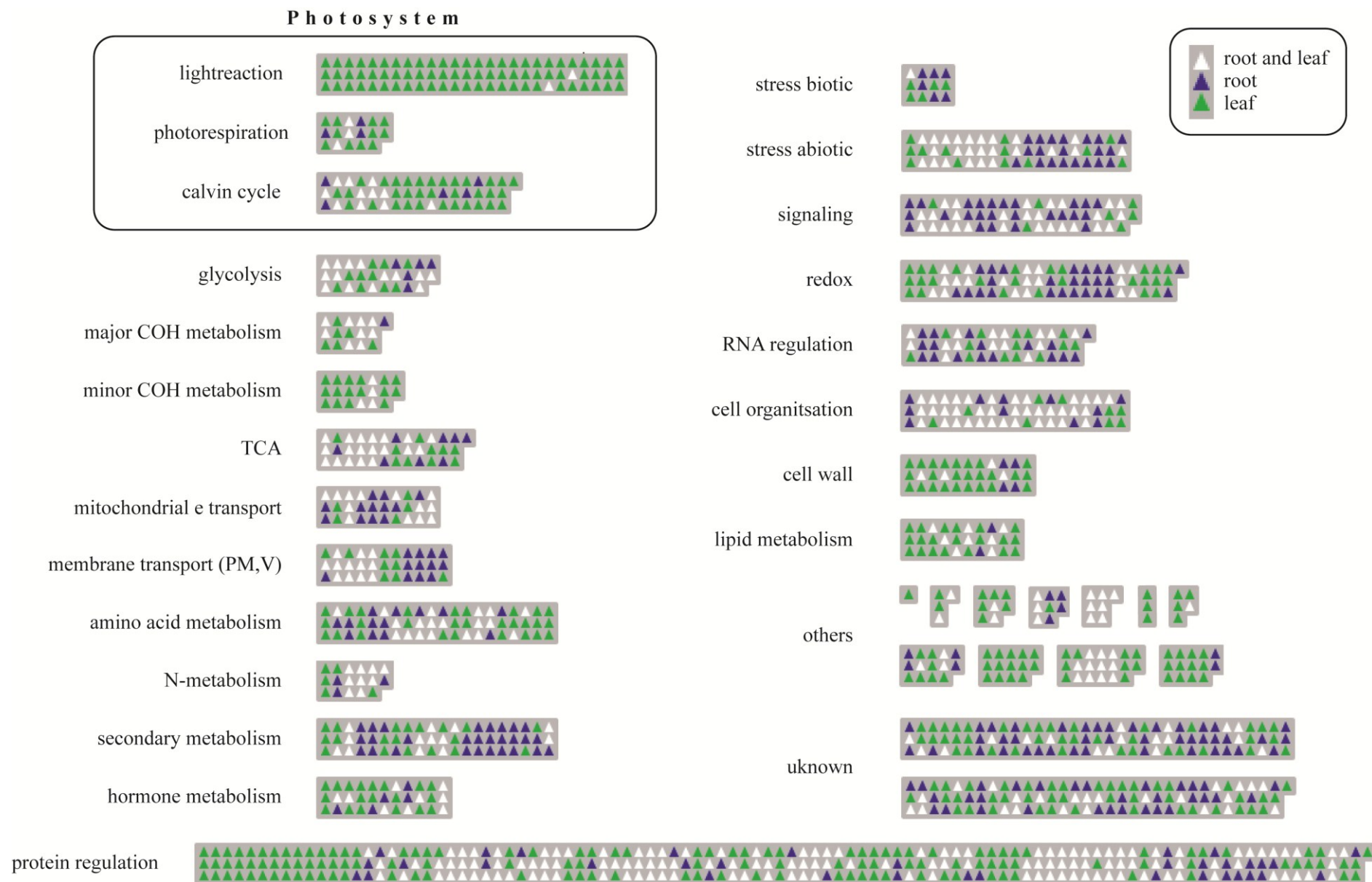


Figure 3.2: Functional distribution of 1521 proteins. The colours indicate the organ proteins derive from.

A principal component analysis (PCA) was done with the COVAIN toolbox, which is designed for uni- and multivariate statistics (Sun & Weckwerth 2012). Proteins with SCs present in less than 4 replicates per treatment were excluded resulting in 845 remaining proteins. Missing values were filled by applying K-nearest neighbor method. The average SCs of each condition was \log^2 transformed and a PCA for root and shoot proteins was performed as shown in fig. 3.3 (a) and (b).

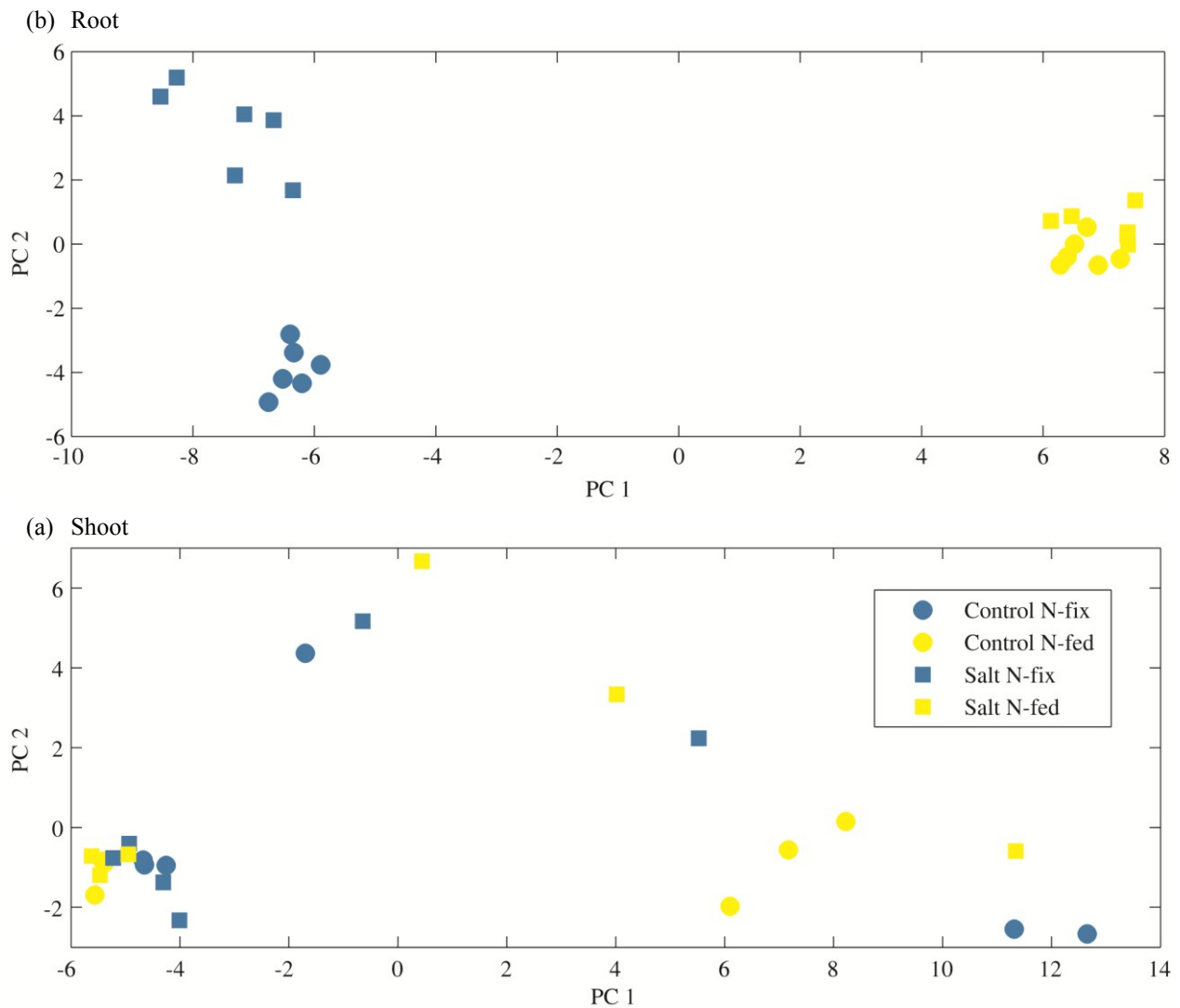


Figure 3.3: PCA-plot of proteomic data of leaves (a) and roots (b). Each treatment shows 6 replicates. Blue spots, N-fix plants; yellow spots: N-fed plants; (a) PC1 explains 48%, PC2 7% of the total variance in the data set. (b) PC1 explains 49%, PC2 7% of the total variance.

The PCA for roots shows clear differentiation: a cluster of each treatment can be identified, whereas principal component 1 (PC1) shows a clear separation of inoculated and fertilized plants. Proteins with the five lowest loadings on PC1 derive from *S. meliloti* which are

nitrogenase iron protein (P00460), leghemoglobin (G7KGT0, P27993), pyruvate dehydrogenase E1 component subunit beta (Q9R9N4) and malate dehydrogenase (Q9EYJ6). Further, PC2 declares the separation of control and stressed plants, whereat stressed N-fed plants show only little variance to control plants compared to N-fix plants. Furthermore, N-fix stressed plants do show higher variance in between the cluster compared to any other treatment, indicating a more diverse response. Replicates of shoot samples do not show clear grouping. Although, the most differences would be expected between inoculated and fertilized plants, shoot-PCA does not lead to such a distinction.

Previous studies (Hoeckenwarter & Wienkoop 2010) have shown that the number of SC of a peptide obtained by high mass accuracy LC/MS/MS (i.e. LTQ-Orbitrap) is a reliable estimate of its relative abundance. Thus, in this work I first characterised all detected proteins and second, given the number of SC's of each peptide, I assessed the significant changes from control to salt stressed plants. The average of SCs per protein of each condition was calculated to determine the up- or down-regulation of each protein. Only proteins with at least 2 fold change (200% up-regulation, 50% down-regulation) and a p-value of less than or equal to 0.05 were considered significant. I found 7% of all identified proteins (108 of 1521) changing significantly during 6 d of salt stress, whereat 70% (76 of 108) of significant changing proteins are localized in the root and 31% (34 of 108) in the shoot. Moreover, 115 proteins of root tissue and 9 proteins found in shoots do show significant differences between N-fix and N-fed control plants making up 8% (124 of 1521) of all identified proteins. Every significant changing protein was categorised accordingly to its function and is listed in A.3-A.4. Categories with little proteins found were combined to the category "others".

A high percentage (15%) of all significant different proteins was putative uncharacterized and was functionally re-annotated performing a BLAST. Putative uncharacterized proteins and the correspondent BLAST results are listed with sequence similarity and E-values in A.3 and A.4. Although only proteins with high BLAST similarities were taken into account, the BLAST of a few proteins resulted in similarities less than 70% for functional categorisation.

When taking a closer look at the tables A.3 and A.4 common stress responding proteins of N-fix and N-fed plants can be found (shown in fig. 3.4). Of all 76 changing proteins in the roots 3 appear to change in both treatments. For leaves, N-fix and N-fed plants only show 1 common protein changing out of 32.

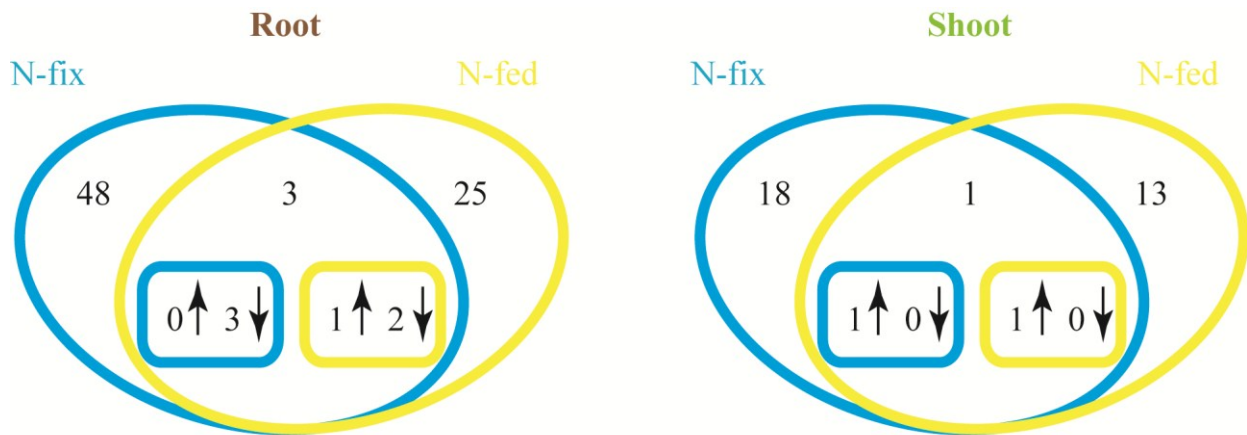


Figure 3.4: Overlap of altering proteins during salt stress for root (3) and shoot (1) respectively. Rectangles indicate up- or down-regulation of common proteins

Arranging all proteins by the treatment, organs and level of expression it can be observed that N-fed plants mainly increase the level of protein expression (28↑,14↓), while response of N-fed plants is almost even in up- and down-regulation (33↑, 27↓). Breaking it down to the organs, N-fed plants most up-regulated proteins are allocated in the leaves (13↑, 1↓). In contrast, N-fix plants mainly decline the level of leaf proteins (4↑, 15↓).

Table 3.2: Protein up- and down-regulation of N-fed and N-fix plants arranged by organs

N-source/organ	altering proteins	up-regulation ↑	down-regulation ↓
N-fix	70	33↑	27↓
- root	51	29↑	22↓
- shoot	19	4↑	15↓
N-fed	42	28↑	14↓
- root	28	15↑	13↓
- shoot	14	13↑	1↓

Concerning the different patterns of up- and down-regulation I further focused on those significant changing proteins which either have similar control levels or similar levels in salt stressed N-fed and N-fix plants (fig. 3.6). For shoot proteins, which have similar control levels, N-fix plants show different expression responds whereas in N-fed plants only up-regulated proteins can be found (except one down-regulation). Root proteins of both nutritional traits show nearly the same number of down-regulated proteins. Concerning similar respond levels in shoots, N-fed plants mainly increased and N-fix plants decreased expression. For root proteins starting at

different control levels neither up- or down-regulation dominates in N-fix or N-fed plants. But symbiotic phenotypes show clearly more regulation in protein expression

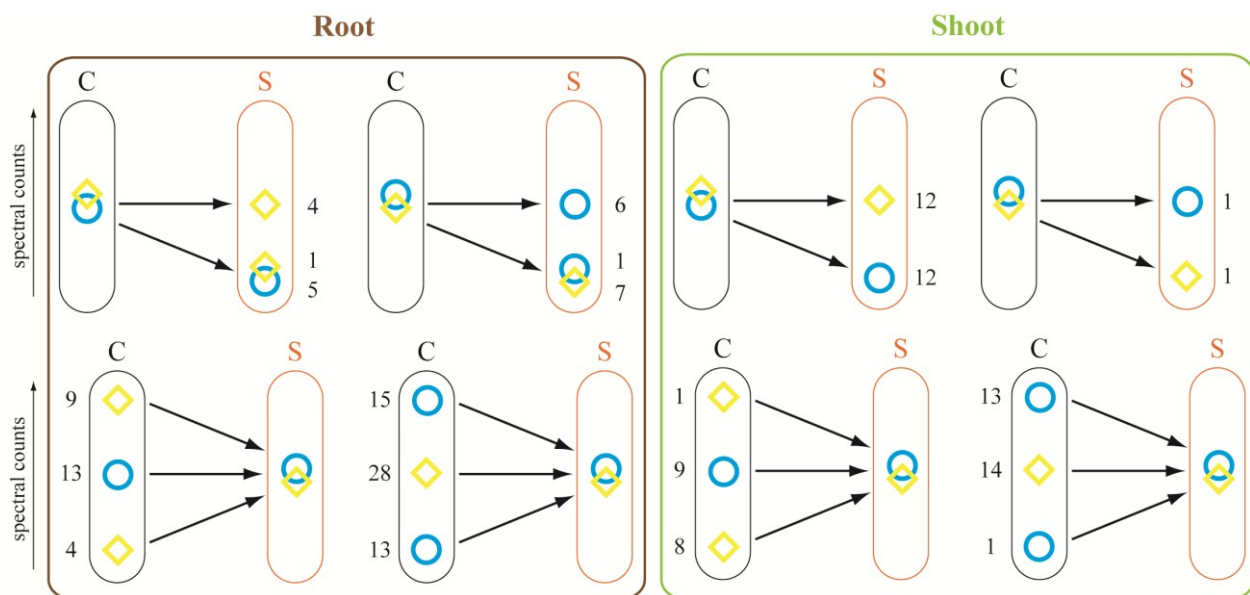


Figure 3.5: Proteins with similar control levels but significant different ($p < 0.05$) stress response (first line) and proteins showing significant different control but similar stress levels (second line)

3.2.1 Normalization of different MS-methods

As described in chapter 2.5 different MS measurement methods were used for half of the technical shoot replicates. The critical difference was the number of dual scans (ms/ms) which was 5 and 10 for each set of replicates respectively. This consequently resulted in a different number of detected peptides and less MS2 scans in dataset 1 as shown in fig. 3.6. However, the replicates did not differ that much in number of full scans compared to the number of MS2 scans. Hence, I analyzed the intensity of precursor m/z in full scans via ProtMAX software (Hoehenwarter et al. 2008) with a target list containing m/z and retention times of peptides obtained by previous MS2 scans in Proteom Discoverer. Due to the differing number of full scans in each set of replicates the data required normalization. Two kinds of normalization were considered: The sum of (a) MS2 scans per sample or (b) all full scans per sample (fig. 3.6). As shown in fig. 3.6 the deviation indicated on the x-axis separates the two sets of replicates. Further the correlation of both datasets is higher on the full scan level compared to MS2 scans confirmed by the coefficient of variance which is 16% on the full scan and 47.4% for MS2 scans. Consequently, normalization of m/z values of each peptide-intensity was achieved through the sum of full scans per sample.

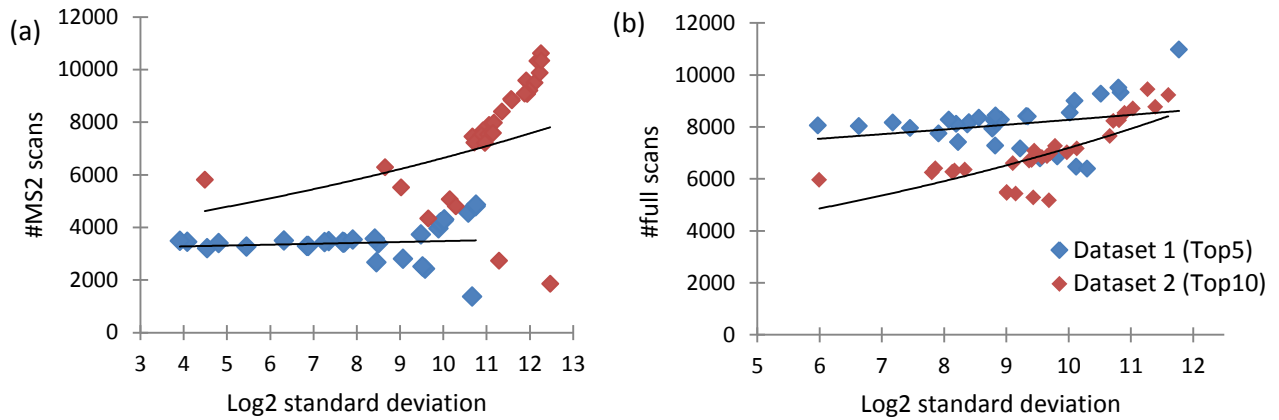


Figure 3.6: Number of (a) MS2 scans and (b) full scans with standard deviation of each sample with regard to both datasets. CV for full scans: 16%, CV for MS2 scans: 47.4%

Analysis of significant changing identified peptides resulted in much less hits (4 peptides listed in A.5) compared to the SEQUEST search algorithm in Proteom Discoverer. One unique peptide, constituting Ferritin, was also found changing by the SEQUEST approach in fertilized plants. Through the MAPA approach, further 3 peptides were found changing significantly.

3.2.2 Root salt stress responsive proteome (see A.3)

Root PCA clearly separates symbiotic and fertilized plants on PC1 mainly because of *S. meliloti* proteins and plant proteins expressed due to symbiotic interaction like leghemoglobin or nodulin which are not expressed in fertilized plants at all (tab. A.3). Furthermore, stressed plants clearly separate from control plants on PC2 showing stronger variance in symbiotic phenotypes. This greater response is confirmed by tab. 3.2 where nearly double as many proteins show alteration in symbiotic roots. Whereat shoot proteome shows counter-correlating up- and down-regulation for N-fed and N-fix plants respectively, the root proteome responded rather balanced (tab.3.2). The root proteome showed 115 proteins significantly changing due to salt stress. Below proteins of the most responding pathways are listed and described.

TCA cycle: The beta subunit E1 of the pyruvate dehydrogenase protein (B7FJJ4) is one out of three units (dihydrolipoyl-transacetylase and dihydrolipoyl-dehydrogenase) making up the pyruvate-dehydrogenase-complex. Its reactive group, the thiazole ring, decarboxylates the pyruvate, which is, after leaving the complex, binding to coenzyme A in form of acetyl to enter the TCA cycle by condensation via citrate-synthase. Acetonitase hydratase (G7ITZ5) catalyzes the isomerization of citrate to isocitrate. Further, a subunit of the cytochrome b-c1 complex (III) (B7FGY5) was decreasing. This complex assembles of 11 subunits of which I detected one altering during stress. It is the third transmembrane complex in the electron transport chain of the oxidative phosphorylation pathway and pumps protons in the intermembrane space. Complex III

oxidises ubiquinon and in this process hands over an electron to cytochrome c. In this pathway the subunit-d (G7I9N0), belonging to the coupling factor F_0 , of the ATP synthase was found up regulating.

Transport: Plasma membrane H^+ -ATPase (G7JUD3), a P-type ATPase is located in the plasma membrane of the mesophyll and root cells where it pumps H^+ out of the cell by ATP usage. H^+ ions are used for nitrate uptake achieved by symport. Nohzadeh Malakshah et al. (2007) suggest a possible role of H^+ -ATPase in adaptation to salt stress. In addition the subunit-c (G7KW90) of a V-type proton ATPase declined. V-type ATPase is located in the tonoplast or the membrane of the golgi apparatus. The number of transported protons per consumed ATP depends on the number of c-subunits the rotor of the F_0 -component contains. The activity of V-ATPase was shown to be according to the metabolic condition through high regulation of the expression of subunits (Ratajczak 2000). Aquaporine PIP11 (G7JB62) did increase. It is a transmembrane protein located in the plasma membrane (PIP...plasma membrane intrinsic protein) responsible for the selective transport of H_2O . It is known that the permeability of aquaporines is self regulated through a built in lit, which responds to the cytosols acidity.

Peroxidase: Two different members of the peroxidase family were found increasing (G8A191, G8A179) another one (G7JUC8) declining. Peroxidases catalyse the reduction of peroxides – mainly H_2O_2 . However, some peroxidases use the reverse reaction to produce H_2O_2 for different reactions. There are many members in the peroxidase family (Welinder et al. 2002) catalyzing a versatility of reactions (Passardi et al. 2005). Peroxidases found catalyse the reaction of 2 molecules phenol and H_2O_2 to 2 phenoxyl radicals plus H_2O . Each peroxidase binds 1 heme B (iron-protoporphyrin IX) and 2 calcium ions per subunit. Peroxidases are known to play an important role in the reinforcement of the cell wall (Fry 2004) as well as heat and salt stress response (Uchida et al. 2002).

3.2.3 Shoot salt stress responsive proteome (see A.4 - A.5)

The shoot proteome showed 35 significantly changing proteins in salt stressed plants located in different compartments. In this section the function of proteins responding to salinity in both nutritional phenotypes are described according to their category.

Mitochondrial electron transport: ATP synthase subunit beta (G7J108) belongs to the catalytic core F_1 , a subunit of ATPase and is located in the inner membrane of chloroplasts and mitochondria. Due to a H^+ -gradient over the membrane ATPase transports protons and synthesizes ATP.

Amino acid metabolism: Four enzymes were found changing in the amino acid metabolism. Alanine aminotransferase (AlaAT, G7JYY7), which catalyses the reaction of L-alanine and α -ketoglutarate to pyruvate and L-glutamate in both directions and thus provides pyruvate for glycolysis or L-alanine for D-alanine metabolism. Hence it is also important for carbon fixation. Further, alanine glyoxylate aminotransferase (G7J014) belongs to the same pathway catalysing glyoxalate and glycine instead of α -ketoglutarate and L-glutamate. Aminomethyltransferase (G7JJ96), located in the cytoplasm, is part of the glycine cleavage system (GCS) which catalyses the degradation of glycine. It is one out of four proteins (P, T, L and H) in the GCS referred to as T-protein, which is the aminomethyl-transferase folate-binding domain. The reaction catalysed by GCS is S(8)-aminomethyldihydrolipoyllysine + tetrahydrofolate to [protein]-dihydrolipoyllysine and 5,10-methylenetetrahydrofolate and NH_3 . The GCS is coupled to the to serine hydroxymethyltransferase (SHMT: $2 \text{ glycine} + \text{NAD}^+ + \text{H}_2\text{O} \rightarrow \text{serine} + \text{CO}_2 + \text{NH}_3 + \text{NADH} + \text{H}^+$). The recycling of glycine through SHMT is a crucial step for glycine oxidation during photorespiration in C3 plants (Douce et al. 2001). GCS and SMHT are reported to be present at high concentration in the mitochondria of pea and spinach leaves (Oliver et al. 1990). Aminomethyltransferase catalyses the degradation of glycine and belongs to the aminotransferases. Further chloroplastic glutamine synthetase leaf isozyme (Q9XQ94) was increasing in both nutritional phenotypes. This enzyme catalyses the binding of ammonia to α -ketoglutarate and is part of the N-metabolism as well as photorespiration.

Cell organization: The tubulin beta chain (G7IAN2, G7IML1, G7JRA0) is the subunit of the dimer tubulin, the major constituent of microtubules. I found three isoforms of the tubulin beta chain changing. Tubulin binds GTP at the exchangeable site on the beta chain and one at a non-exchangeable site on the alpha-chain. Microtubules contribute to maintenance of cell structure, intracellular transport and cell division.

Metal handling: I found three different isoforms of ferritin (G7JLS7, G7K283, A5HKJ9). It was found that its peptide pre-sequence suggests chloroplast targeting. However, there is a high potential that ferritin could be dual targeted to both plastids and mitochondria (Zancani et al. 2004). Its function is the storage of iron in a soluble, non-toxic and readily available form. It is involved in the porphyrin and chlorophyll metabolism and hence important for protein homeostasis. Ferritin is known to avoid oxidative stress by iron sequestration (Ravet et al. 2009).

4. Discussion

Research on plant response to salt and drought stress gained importance during the past decades (Parida & Das 2005, Tardieu 2012). Especially the awareness of a forthcoming climate change led to deeper research on agricultural crop plants. Approaching this problem from a molecular view allows the integration of new methods for designing better adapted plants (Weckwerth 2011a, Bartels & Nelson 1994). In this experiment a moderate stress level of salt and drought stress was applied to *Medicago truncatula* under different nitrogen sources in order to assess the proteomic stress response. To compare the different stresses on an organism level, plants were harvested at the same age after 6 days of either water deprivation or salt stress (200 mM). For the evaluation of the stress degree, the plants water status was analysed through different physiological parameters. In this work I specified the differential physiological response to salt and drought stress. Furthermore, I determined salt stress responsible proteins and suggest the probable metabolic response of root and shoot with regard to physiological characterisation.

4.1. Stress determination and physiological response

Physiological parameters clearly show that plants were exposed to severe water and salt stress. Photosynthesis was limited due to CO₂-fixation as stomatal conductance was declining to a minimum, whereas the response in symbiotic salt stressed plants was stronger compared to drought stressed ones. Furthermore, the leaf water potential significantly declined in drought stressed plants, whereas salt stressed plants maintained their leaf water status. This might be due to the more significant stomatal closure controlled by an increased ABA level in the root xylem (Tardieu et al. 1992). Records of the leaf water content support the measurements of leaf water potential as only the leaf water content of drought stressed plants declined. However, this significant decline was only observed in fertilized plants. Regarding the specific leaf area (SLA), an indicator for leaf thickness, again only drought stressed plants show changes whereas symbiotic plant's specific leaf area is lower compared to control plants which counter correlates with fertilized plants showing a lower SLA. There were no significant changes observed in salt stressed plants indicating that leaf water status was not affected that much. This suggests more severe effects to drought than to salt stress. Moreover, fertilized plants generally had a greater specific leaf area and also higher reduction in soil water content during drought stress. SLA in drought stressed symbiotic plants slightly but significantly increased whereas fertilized plants show a decrease in SLA. In relation to the LWC it can be concluded that fertilized plants lose more water during drought stress whereas in symbiotic plants less alteration was observed in SLA, LWC

and Ψ_T . However, leaves of N-fed plants were observed to die off sooner. Furthermore, until the time of measurement, fertilized plants DW was three times the DW of symbiotic plants what consequently might result in additional water uptake. To minimize effects of different plant dimensions on water uptake, the method of irrigation can be changed. During drought stress, the volume of remaining nutrient solution in the pot might be adapted to the littlest amount of nutrient solution absorbed by a plant on a daily base. Thus, it can be ensured that the soil water content decreases proportionally in all pots.

Looking on how DW alters during drought stress, it can be observed that unexpectedly symbiotic plants gained weight. A set of 6 replicates can prevent such a coincident. The very different growth performance in symbiotic plants might be due to inoculation problems. An earlier time point of inoculation may increase the number of nodules per plant and 3 times of inoculation may increase the chance of successful rhizobial formation. However, still a significant difference of growth performance between N-fed and N-fix plants can be observed making comparison of plants during drought stress more difficult. Inoculation with *S. medicae* was reported to perform better in terms of growth (Terpolilli et al. 2008) making symbiotic plants more comparable with N-fed ones.

Alteration of electrical conductivity of the leaves as well as the substrate and the osmotic potential were measured on salt stressed plants and a subset of controls as these parameters are only important with regard to ion uptake. Salt stressed plants did show a significant higher Ψ_s . In short, they are increasing osmotic potential, which is known to be achieved by either dissolved ions or other osmotic active molecules (e.g. sugars). According to Larcher (2011) irrigation water should not exceed EC of 2 mS/cm. In our case nutrient solutions EC was at 0.419 mS/cm. This resulted in a significant increase of ions in salt stressed plants compared to controls. EC in the substrate increased nearly four times showing that accumulation of ions was higher in the substrate than in the leaves. Nevertheless, ions still need to be determined in composition as the question arises whether NaCl is taken up by the plants with nutrient solution, or if plants manage to absorb water only. If so, it still needs to be determined to what degree plants are able to absorb water only. Our data indicates that plants being stressed for six days with 200 mM NaCl nutrient solution are still capable of efficient water uptake. Munns (2002) suggested a two-phase growth response to salt stress where the initial growth reduction is due to osmotic effects in the substrate as well as probable hormone signals deriving from the roots. During this initial phase the response to salt or drought stress are alike. In our experiment reduction in growth was not yet ob-

served after 6 d. The differentiation of salt-sensitive to salt-tolerant plants is the ability to prevent salt reaching toxic levels constraining the metabolism (Sanchez et al. 2008). To assess the physiological threshold where the concentration of ions in leaves starts being toxic prolonged salt stress with analysis of growth and leaf area is necessary. For the investigation of the osmotic adaption in leaves the determination of ion composition, especially sodium and chlorine, is required.

4.2. Complicated data mining of different MS-methods

The PCA of shoots did not show great variance in the nutritional traits or the stressed plants. This is mainly due to the different measurement methods (shown in fig. 3.6). To compensate this imbalance of SC in shoot data I normalized by the sum of full scans per sample. Subsequently MAPA was performed to obtain differences of ion intensities on the peptide level. The advantages of the ProtMAX software were not used for additional peptide determination (db-independent). Nevertheless, a db-independent approach would enable an assignment of quantitative differences of peptides on the full scan level as well as further investigation of peptide isoforms and modification. Oxidised methionine is such a modification and was detected in this research in the peptide with m/z 729.33 (aa-sequence is provided in table A.5). A student's T-test was performed on protein and peptide data to assign significant differences in control and stressed phenotypes. Further, only two fold differences in protein SC or ion intensity for peptides were considered. Due to performed MAPA the differences in MS2 scans were minimized. Nevertheless, different methods of measurement in between one set of samples will be avoided in future experiments.

4.3. Proteome stress modifications depending on nutritional phenotypes

4.3.1 Shoot proteome

By assessing protein alteration from a regulatory view I discovered response patterns related to the different nutritional traits. Those patterns are based on different control levels. Table A.2. shows 10 proteins with significant higher expression in control levels of N-fix compared to N-fed phenotypes. One out of these proteins (ferritin) was found responding to salt stress. In addition, concerning altering proteins due to stress tab.3.2 shows dominating down-regulation in N-fix plants whereas N-fed plants nearly completely up-regulate protein expression. Figure 3.6

emphasizes this pattern of a counter-correlating up- and down-regulation ratio in symbiotic and fertilized phenotypes. Staudinger et al. (2012) confirmed this pattern by additional measurements of metabolites of salt stressed phenotypes. In addition, they found similar response patterns to drought stress.

Fig. 3.4 shows an overlap of one protein in both nutritional phenotypes due to salt stress: chloroplastic glutamine synthetase leaf isozyme. This enzyme is involved in the amino acid metabolism in which I found 2 further proteins (G7JYY7, G7JJ96) down-regulated in N-fix plants and one (G7J014) up-regulated in N-fed phenotypes in response to stress. Thus, the amino acid metabolism is one of the most responding cell activities which I discuss subsequently. Additionally, tubulin was increasing in both nitrogen traits. Cell organisation was reported to play an important role in stress response (Wang et al. 2007, Wang et al. 2011, Zhang et al. 2012). Hence, I go into discussion with tubulin as major agent of the cytoskeleton.

Amino acid modifying proteins involved in photorespiration

The *alanine aminotransferase* (G7JYY7) was found decreasing in stressed symbiotic plants. According to Ricoult et al. (2006) there are four different AlaAT expressed in the mitochondria and the cytosol of leaf, stem and root tissue. AlaAT is being studied as responsible enzyme for hypoxic tolerance in *A. thaliana*, *G. max* and *M. truncatula* (Miyashita et al. 2007, Ricoult et al. 2006, Rocha et al. 2010). Hypoxia mainly occurs due to waterlogging which is especially risky for seedlings. Rocha et al. (2010) suggest AlaAT responsible for catabolism of alanine during the initial period of re-oxygenation.

Alanine glyoxylate aminotransferase (G7J014) a photorespirational enzyme increased during stress. It catalyses the reaction of glyoxylate and alanine to glycine and pyruvate. Glycine is further processed in the pathway of the photorespiration. *aminomethyltransferase* was found declining. It is part of the GCS, also known as the glycine decarboxylase complex, and as well belongs to the photorespiration pathway catalysing the cleavage of glycine to produce serine for further recycling to 3-phosphoglycerate. In this reaction ammonia and CO₂ are side products. Loss of ammonia is prevented by glutamine synthetase.

The common up-regulation of the chloroplastic *glutamine synthetase* leaf isozyme (Q9XQ94) with regard to the strong stomatal closure in both nutritional phenotypes indicates severe stress and ongoing photorespiration. If stomata are closed declining of CO₂ partial pressure leads to increased binding of rubisco to O₂. Due to this, less ribulose-1,5-bisphosphate is recovered in the

Calvin-cycle resulting in higher concentrations of 2-phosphoglycolat. The recycle process of 2-phosphoglycolat includes the catalysis of two molecules glycine to serine in which ammonia and CO₂ are produced. To regain valuable nitrogen, ammonia is bound to glutamate to form glutamine. Its amino group is subsequently bound to α -ketoglutarate resulting in 2 molecules glutamate. Many metabolic reactions are included in the photorespiration being performed in chloroplasts, peroxisomes and mitochondria. A bottleneck of photorespiration seems to be the glutamine synthetase (Häusler et al. 1994, Wallsgrove et al. 1987). Hoshida et al. (2000) found enhanced salt tolerance in rice plants that overexpressed glutamine synthetase in chloroplasts suggesting that the reuptake of ammonia is vital for plant survival during salt stress. However, not only ammonia might be crucial in photorespiration during stress. But photorespiration itself is a possible route for dissipation of excess light energy or reducing power (Brisson et al. 1998). Thus it prevents the over-reduction of the electron transport chain which causes the generation of ROS (Osmond & Grace 1995).

Cell organisation

Tubulin beta chains (G7IAN2, G7IML1, G7JRA0) raised in all stressed phenotypes to four times the control level and represents a non nutritional specific response. Although different isoforms were found changing, all indicate similar response to salt stress in the cytoskeleton. Wang et al. (2007) found rapid depolymerisation of microtubule (MT) due to salt stress and suggested that a corticale reorganization of the MT network is better suited for high salinity. Zhang et al. (2012) suggested a functional connection between a plasma membrane protein and MT associated protein showing environmental stress signaling. Further, it was proposed by Wang et al. (2007) that the depolymerisation of corticale MT regulates calcium channel activity. This increase of Ca²⁺ is then important for the reorganisation of corticale MT. Calcium is known to activate SOS3 (salt overly sensitive) thus initialising a signalling cascade which leads to increased expression of antiporter and activation of Na⁺/H⁺ antiporter (Hasegawa & Bressan 2000).

4.3.2 Root proteome

Proteins altering in both nutritional treatments belong to the categories cell wall proteins, lipid metabolism and metal handling. A cell wall protein - UDP-glucose 6-dehydrogenase (G7L571), intermediating hemicellulose and pectin synthesis - declined. Studies of Iraki (Iraki et al. 1989a, Iraki et al. 1989b) found that salt stress inhibits cell wall metabolism and stressed cells have con-

siderable less tensile strength. One protein of the lipid metabolism - Phospholipase D (Q2HUA3) - responded decreasing. Phospholipase D is known to be regulated by calcium in response to various stressors (Wang 2002). And S-adenosylmethionine synthase (SAMS, Q6J9X6), a universal methyl-group donor, shows up- and down-regulation in N-fix and N-fed phenotypes respectively, whereat the stress level in N-fed plants is equivalent to the one of symbiotic controls. SAMS is reported to be induced by salinity in the roots of tomato plants (Espartero et al. 1994, Sánchez-Aguayo et al. 2004). Of all significant altering root proteins being categorised our attention was drawn to two groups showing alteration mainly in one of the nutritional phenotypes. Additionally, different control levels of those groups indicate nutrient specific response. Hence, in the following I will discuss peroxidase and transport proteins altering due to salinity exposure.

Peroxidase

Class III *Peroxidases* (POD) do have many features (Passardi et al. 2005) whereat with regard to stress the most important tasks are the reinforcement of the cell wall and protection of the plasma membrane through ROS-scavenging. In rice seedlings root growth was reported to decrease during osmotic stress (150 mM NaCl) correlating with increased levels of H₂O₂ and POD after 16 h of treatment (Lin & Kao 2001). Furthermore, Wang et al. (2009) suggested that elevated POD activity in roots reflect increased ROS scavenging capacity and decreased damage to lipids of the plasma membrane under stress. By comparing salinity tolerant and sensitive alfalfa varieties he found that origin POD levels are lower in sensitive cultivars. Increased tolerance to salt stress in plants with higher POD activity was found in tomatoes (Shalata & Tal 1998) and *Plantago maritima* (Sekmen et al. 2007). Higher levels of POD were also reported to play an important role in drought stress of common bean (Türkan et al. 2005), sunflower and sorghum (J. Zhang & Kirkham 2006). Our results show ~60% higher POD levels (G8A191, G8A179) in fertilized plants increasing three fold from origin levels (one isoform responded decreasing; G7JUC8) during salt stress whereas symbiotic plants do not show significant differences in POD expression. Hence, I suggest an initial nutritional phenotype specific expression of POD in roots and subsequently a stress specific response to elevated levels of H₂O₂. However, increasing levels of H₂O₂ remain to be determined.

Transport

Plasma membranes (PM) have a negative biochemical potential. Thus, exposed to salinity sodium flows towards this gradient. The imbalance of ions caused by increased Na^+ uptake results in the destruction of the PM. The flood of sodium into the cytosol further positively effects the activity of proton pumps especially ATPases in the PM and the tonoplast to re-obtain ion homeostasis. Niu et al. (1993) found mRNA of *PM-H⁺-ATPase* in halophytes accumulating greater than in glycophytes in respond to elevated salinity indicating that organs require increased H^+ electrochemical potential. However, it was found by Rabhi et al. (2007) that elevated salinity associated with limited Fe availability resulted in diminishing root acidification. However, other studies stated exceptions to this rule as *PM-H⁺-ATPase* was found decreasing in wheat (Raven 1986) and tomatoes - variety dependent (Sanchez-Aguayo et al. 1991). Here I found *PM-H⁺-ATPase* (G7JUD3, G7JUD2) of both nutritional phenotypes declining in respond to elevated salinity.

Through prolonged salt stress, sodium is transported to the vacuole to retain cytosolic ion homeostasis (Binzel et al. 1988) resulting in an alkalisation of the vacuole due to proton-sodium antiport. Dietz et al. (2001) suggested that the survival of cells during stress conditions strongly depends on the adjustment of V-ATPase. In our experiment, the expression of the *V-ATPase subunit c* (G7KW90) was about a third compared to control levels. The number of c-subunits the rotor of the F_0 -component contains affects the number of transported protons per consumed ATP (Sambongi 1999). Furthermore, the different expression of subunit c genes was reported to play a role in *A. thaliana* (Padmanaban et al. 2013) and *Mesembryanthemum crystallinum* (Tsiantis et al. 1996) in salt regulation. Studies of Otoch et al. (2001) with hypocotyls of seedlings of the legume *Vigna unguiculata* under salt stress showed a decrease of proton transport activities in the vacuole after 3 days, whereas after 7 days proton transport activities were higher. Likewise, Wang et al. (2000) found V-ATPase of wheat roots decreasing after 3 days by a factor of 2.4 due to elevated salinity (200 mM). In this study as well subunits of the V-ATPase (G7KW90, Q2HUI7) were decreasing in N-fix plants after extended salt stress of 6 days. However, no subunit of V-ATPase in fertilized plants was responding to salt treatment indicating a stronger and thus more specific reaction in symbiotic plants.

Two proteins of the *aquaporine* family (O22339, G7JB62) increased 3 and 4 times in roots of symbiotic plants due to 6 days stress exposure. The first protein, which is only evident at tran-

script level, can not be further classified to any subgroup of aquaporines but shows high similarity to the second responding aquaporin belonging to the plasma membrane intrinsic proteins (PIP) class 11 aquaporines. PIP1 aquaporines are reported to contribute to the hydrostatic pressure in roots and rosette of *A. thaliana* (Postaire et al. 2010). Aquaporines in generally are found increasing in roots of *alfalfa* due to elevated salinity (Jang et al. 2004), whereas to dehydration non-nodulated roots of *alfalfa* responded with down regulation of aquaporines (Chen et al. 2007). Research by Jang et al. (2004) showed that in roots of 2 weeks old *A. thaliana* seedlings the PIP1 class aquaporines responded with a 5 fold increase due to salt stress. Recently Hu et al. (2012) found enhanced salt tolerance in wheat overexpressing aquaporine PIP1 which increased root elongation and further retained high Ca^+ content and K^+/Na^+ ratio. They found reduced H_2O_2 accumulation and in accordance to this work alteration of peroxidases in fertilized plants. In this experiment, N-fix phenotypes increased expression of aquaporines with no associated regulation of peroxidases.

5. Summary

Nitrogen fixing bacteria evolved very early on an evolutionary time scale. Thus the symbiosis with plants became crucial for the survival of both partners. All members of the legumes form so called root nodule housing rhizobia enabling them to uptake atmospheric nitrogen. As natural soil fertilizers and protein rich nutrition many legume species became important crop plants (e.g. pea, bean). Natural ecosystems as well as agriculture are facing climate change the next decades which demands for drought and salt tolerant varieties. Studies on diverse abiotic stress factors were already done but they still leave open questions on how symbiotic plants respond to stress with their partner. To approach this question the legume model organism *Medicago truncatula* was fertilized or inoculated with *Sinorhizobium meliloti* and exposed to 6 days of either drought or salt stress. Physiological assessments showed that all stress types affected the plants water status confirming moderate stress level. Stomatal closure was higher and water potential was maintained in salt but not in drought stressed plants indicating higher tolerance to salt stress. This was confirmed by unchanged specific leaf area and stable water potential during salt exposure. Specific leaf area and leaf water content showed less alteration in symbiotic plants while water deprivation indicating nutritional related response. The shoot and root proteome of salt stressed phenotypes was analysed for further stress respond specification. The shoot proteome showed nutrient dependent response patterns which were counter-correlating in symbiotic and fertilized plants. All stressed phenotypes shared ongoing photorespiration by showing increased levels of glutamine synthetase. Further, greater tubulin expression in shoots confirms that the reorganisation of the cytoskeleton is a central adjustment to salinity. Principal component analysis of the root proteome showed variance between control and salt treated plants. Roots proteome revealed clear differences of peroxidase levels between the nutritional traits showing three fold higher expressions in fertilized control plants. A common respond of nutritional phenotypes was observed in a decrease of plasma membrane H^+ -ATPase. A specific nutritional dependent reaction of roots was found with the decrease of a V-ATPase subunit in nodulated plants. Respond of transport proteins further involved a fourfold increase of aquaporines only in symbiotic plants. Altogether, the proteome analysis in this work provides evidence for a nutrient specific salt stress response of *Medicago truncatula* and additionally suggests responsible pathways.

6. Zusammenfassung

Die Evolution von stickstofffixierenden Bakterien begann sehr früh und die Symbiose mit Pflanzen war entscheidend für das Fortbestehen beider Partner. Mitglieder der Leguminosen bilden Wurzelknöllchen, welche Rhizobien beherbergen die ihren Partner mit Stickstoff versorgen. Durch diese natürlicher Bodendüngung und proteinreiche Samen sind Leguminosen wichtige Erntepflanzen (zB. Erbsen, Bohnen). Da der Weltbevölkerung ein nahender Klimawandel bevorsteht wird nach neuen Züchtungen, die besonders stresstolerant sind, nachgefragt. Zahlreiche Studien über verschiedene abiotische Stressfaktoren wurden durchgeführt, ließen aber die Frage offen, wie symbiotische Pflanzen im Zusammenspiel mit ihrem Partner reagieren. Um diese Frage zu beantworten, setzten wir gedüngte oder inokulierte Pflanzen des Modellorganismus *Medicago truncatula* für sechs Tage Trocken- oder Salzstress aus. Unsere physiologische Bewertung zeigte, dass beide Stressarten den Wasserhaushalt der Pflanzen beeinflusste und bestätigt somit ein moderates Stresslevel. Stärkerer Stomatenschluss, gleichbleibendes Wasserpotenzial und spezifische Blattfläche zeigten leichtere Adaption bei erhöhten Salzkonzentrationen, während bei Trockenstress das Wasserpotenzial sank. Spezifische Blattfläche und Blattwassergehalt änderten sich in Symbionten bei Trockenstress weniger stark, was auf eine Nährstoff bedingte Reaktion schließen lässt. Das Spross- und Wurzelproteom von salzgestressten fertilisierten und inokulierten Pflanzen wurde auf seine Stressantwort analysiert. Das Sprossproteom zeigte gegengleich reagierende Muster in fertilisierten und symbiontischen Phenotypen. Alle gestressten Pflanzen hatten andauernde Photorespiration gemeinsam, welche besonders an erhöhter Expression von Glutaminsynthetase erkennbar war. Die hohe Tubulinexpression im Sprossproteom bestätigte, dass die Reorganisation des Zytoskelets eine zentrale Anpassung in Bezug auf Salzstress ist. Die Hauptkomponentenanalyse des Wurzelproteoms zeigte eine Auftrennung von Kontrollpflanzen und Salzstress ausgesetzten Pflanzen und ließ klare Unterschiede bei Peroxidasen zwischen den verschiedenen Nährstoffbedingungen erkennen. Beide Nährstoff-Phenotypen reagierten gleich mit einem Abfall an Plasmamembran H^+ -ATPase. Eine Symbionten spezifische Antwort zeigte sich bei der Abnahme einer V-ATPasen Untereinheit. Die Stressantwort von Transportproteinen umfasste zudem einen vierfachen Anstieg von Aquaporinen in symbiontischen Pflanzen. Die Proteomanalyse in dieser Arbeit zeigt somit eine nährstoffabhängige Stressantwort von *Medicago truncatula* auf erhöhte Salinität und gibt Hinweise auf verantwortliche Signalwege.

7. Bibliography

- Almeida, J.P. et al., 2000. Evidence that P deficiency induces N feedback regulation of symbiotic N₂ fixation in white clover (*Trifolium repens* L.). *Journal of experimental botany*, 51(348), pp.1289–97.
- Arabidopsis, T. & Initiative, G., 2000. Analysis of the genome sequence of the flowering plant *Arabidopsis thaliana*.
- Bartels, D. & Nelson, D., 1994. Approaches to improve stress tolerance using molecular genetics. *Plant, Cell and Environment*, 17(5), pp.659–667.
- Bell, C.J. et al., 2001. The Medicago Genome Initiative: a model legume database. *Nucleic acids research*, 29(1), pp.114–7.
- Binzel, M.L. et al., 1988. Intracellular compartmentation of ions in salt adapted tobacco cells. *Plant physiology*, 86(2), pp.607–14.
- Bradford, M.M., 1976. A rapid and sensitive method for the quantitation of microgram quantities of protein utilizing the principle of protein-dye binding. *Analytical biochemistry*, 72, pp.248–54.
- Brisson, L.F., Zelitch, I. & Havir, E. a, 1998. Manipulation of catalase levels produces altered photosynthesis in transgenic tobacco plants. *Plant physiology*, 116(1), pp.259–69.
- Cantacessi, C. et al., 2010. A practical, bioinformatic workflow system for large data sets generated by next-generation sequencing. *Nucleic acids research*, 38(17), pp.171–172.
- Carpentier, S.C. et al., 2005. Preparation of protein extracts from recalcitrant plant tissues: an evaluation of different methods for two-dimensional gel electrophoresis analysis. *Proteomics*, 5(10), pp.2497–507.
- Del Castillo, L.D., Hunt, S. & Layzell, D.B., 1994. The Role of Oxygen in the Regulation of Nitrogenase Activity in Drought-Stressed Soybean Nodules. *Plant physiology*, 106(3), pp.949–955.
- Chen, D. et al., 2007. Identification of dehydration responsive genes from two non-nodulated alfalfa cultivars using Medicago truncatula microarrays. *Acta Physiologiae Plantarum*, 30(2), pp.183–199.
- Coelho, S.M. et al., 2007. Complex life cycles of multicellular eukaryotes: new approaches based on the use of model organisms. *Gene*, 406(1-2), pp.152–70.
- Cook, D.R., 1999. Medicago truncatula - a model in the making ! Commentary. *Current opinion in plant biology*, 2(4), pp.301–304.

- Corwin, D.L. & Lesch, S.M., 2005. Apparent soil electrical conductivity measurements in agriculture. *Computers and Electronics in Agriculture*, 46(1-3), pp.11–43.
- Dietz, K.J. et al., 2001. Significance of the V-type ATPase for the adaptation to stressful growth conditions and its regulation on the molecular and biochemical level. *Journal of experimental botany*, 52(363), pp.1969–80.
- Douce, R. et al., 2001. The glycine decarboxylase system: a fascinating complex. *Trends in plant science*, 6(4), pp.167–76.
- Eng, J.K., McCormack, A.L. & Yates, J.R., 1994. An Approach to Correlate Tandem Mass Spectral Data of Peptides with Amino Acid Sequences in a Protein Database. *American Society Mass Spectrometry*, 5, pp.976–989.
- Espartero, J., Pintor-Toro, J.A. & Pardo, J M, 1994. Differential accumulation of S-adenosylmethionine synthetase transcripts in response to salt stress. *Plant molecular biology*, 25(2), pp.217–27.
- Evans HJ, 1981. Symbiotic nitrogen fixation in legume nodules. In M. TC, ed. *Research Experiences in Plant Physiology*. New York: Springer-Verlag, pp. 294–310.
- Fry, S.C., 2004. Primary cell wall metabolism : tracking the careers of wall polymers in living plant cells. *New Phytologist*, 161, pp.641–675.
- Gálvez, L., González, E.M. & Arrese-Igor, C., 2005. Evidence for carbon flux shortage and strong carbon/nitrogen interactions in pea nodules at early stages of water stress. *Journal of experimental botany*, 56(419), pp.2551–61.
- Gardner, Catriona M.K., David Robinson, Ken Blyth, J.D.C., 2000. Soil Water Content. In C. E. M. Keith A. Smith, ed. *Soil and Environmental Analysis - Physical Methods*. New York: Marcel Dekker, pp. 2–9.
- Harlan, J.R., 1992. *Crops and man* 2nd editio., American Society of Agronomy.
- Hasegawa, Paul M & Bressan, R.A., 2000. Plant cellular and molecular responses to high salinity. *Annual review of plant physiology and plant molecular biology*, 51, pp.463–499.
- Häusler, R., Lea, P.J. & Leegood, R.C., 1994. Control of photosynthesis in barley leaves with reduced activities of glutamine synthetase or glutamate synthase II . Control of electron transport and CO₂ assimilation. , pp.418–435.
- Hoehenwarter, W. et al., 2008. A rapid approach for phenotype-screening and database independent detection of cSNP/protein polymorphism using mass accuracy precursor alignment. *Proteomics*, 8(20), pp.4214–25.
- Hoehenwarter, W. & Wienkoop, S., 2010. Spectral counting robust on high mass accuracy mass spectrometers. *Rapid Communications in Mass Spectrometry*, pp.3609–3614.

- Hoshida, H. et al., 2000. Enhanced tolerance to salt stress in transgenic rice that overexpresses chloroplast glutamine synthetase. *Plant molecular biology*, 43(1), pp.103–11.
- Hu, W. et al., 2012. Overexpression of a Wheat Aquaporin Gene, TaAQP8, Enhances Salt Stress Tolerance in Transgenic Tobacco. *Plant & cell physiology*, 53(12), pp.2127–2141.
- Iraki, N. et al., 1989a. Alteration of the physical and chemical structure of the primary cell wall of growth-limited plant cells adapted to osmotic stress. *Plant physiology*, 91(1), pp.39–47.
- Iraki, N.M., Bressan, R. a & Carpita, N.C., 1989b. Extracellular polysaccharides and proteins of tobacco cell cultures and changes in composition associated with growth-limiting adaptation to water and saline stress. *Plant physiology*, 91(1), pp.54–61.
- Jang, J.Y. et al., 2004. An expression analysis of a gene family encoding plasma membrane aquaporins in response to abiotic stresses in *Arabidopsis thaliana*. *Plant molecular biology*, 54(5), pp.713–25.
- Larcher, W., 2011. *Ökophysiologie der Pflanzen*, 6th ed., Stuttgart: UTB.
- Larrainzar, Estíbaliz et al., 2009. Carbon metabolism and bacteroid functioning are involved in the regulation of nitrogen fixation in *Medicago truncatula* under drought and recovery. *Molecular plant-microbe interactions : MPMI*, 22(12), pp.1565–76.
- Larrainzar, Estíbaliz et al., 2007. *Medicago truncatula* root nodule proteome analysis reveals differential plant and bacteroid responses to drought stress. *Plant physiology*, 144(3), pp.1495–507.
- Lin, C.C. & Kao, C.H., 2001. Absciscic acid induced changes in cell wall peroxidase activity and hydrogen peroxide level in roots of rice seedlings. *Plant science : an international journal of experimental plant biology*, 160(2), pp.323–329.
- Markmann, K., Giczey, G. & Parniske, M., 2008. Functional adaptation of a plant receptor-kinase paved the way for the evolution of intracellular root symbioses with bacteria. *PLoS biology*, 6(3), pp.497–506.
- Miyashita, Y. et al., 2007. Alanine aminotransferase catalyses the breakdown of alanine after hypoxia in *Arabidopsis thaliana*. *The Plant journal : for cell and molecular biology*, 49(6), pp.1108–21.
- Munns, R., 2002. Comparative physiology of salt and water stress. *Plant, cell & environment*, 25(2), pp.239–250.
- Niu, X. et al., 1993. NaCl regulation of plasma membrane H(+)-ATPase gene expression in a glycophyte and a halophyte. *Plant physiology*, 103(3), pp.713–8.
- Nohzadeh Malakshah, S. et al., 2007. Proteomics Reveals New Salt Responsive Proteins Associated with Rice Plasma Membrane. *Bioscience, Biotechnology, and Biochemistry*, 71(9), pp.2144–2154.

- O'Neal, M.E., Landis, D. a & Isaacs, R., 2002. An inexpensive, accurate method for measuring leaf area and defoliation through digital image analysis. *Journal of economic entomology*, 95(6), pp.1190–4.
- Ojciechowski, M.A.F.W., Avin, M.A.T.T.L. & Anderson, M.I.J.S., 2004. A phylogeny of legumes (Leguminosae) based on the analysis of the plastid MATK gene resolves many well-supported subclades within the family. *American Journal of Botany*, 91(11), pp.1846–1862.
- Oliver, D.J. et al., 1990. Interaction between the Component Enzymes of the Glycine Decarboxylase Multienzyme Complex. *Plant physiology*, 94(2), pp.833–9.
- Osmond, C.B. & Grace, S.C., 1995. Perspectives on photoinhibition and photorespiration in the field: quintessential inefficiencies of the light and dark reactions of photosynthesis? *Journal of Experimental Botany*, 46, pp.1351–1362.
- Otoch, M.D.O. et al., 2001. Salt modulation of vacuolar H⁺-ATPase and H⁺-Pyrophosphatase activities in *Vigna unguiculata*. *Journal of Plant Physiology*, 158, pp.545–551.
- Padmanaban, S. et al., 2013. Differential Expression of Vacuolar H⁺-ATPase Subunit c Genes in Tissues Active in Membrane Trafficking and Their Roles in Plant Growth as Revealed by RNAi. *Plant Physiology*, 134, pp. 1514-1526.
- Parida, A.K. & Das, A.B., 2005. Salt tolerance and salinity effects on plants: a review. *Ecotoxicology and environmental safety*, 60(3), pp.324–49.
- Passardi, F. et al., 2005. Peroxidases have more functions than a Swiss army knife. *Plant cell reports*, 24(5), pp.255–65.
- Platt, A. et al., 2010. The scale of population structure in *Arabidopsis thaliana*. *PLoS genetics*, 6(2), p.e1000843.
- Postaire, O. et al., 2010. A PIP1 aquaporin contributes to hydrostatic pressure-induced water transport in both the root and rosette of *Arabidopsis*. *Plant physiology*, 152(3), pp.1418–30.
- Rabhi, M. et al., 2007. Interactive effects of salinity and iron deficiency in *Medicago ciliaris*. *Comptes rendus biologiques*, 330(11), pp.779–88.
- Ratajczak, R., 2000. Structure, function and regulation of the plant vacuolar H⁽⁺⁾-translocating ATPase. *Biochimica et biophysica acta*, 1465(1-2), pp.17–36.
- Raven, B.Y.J.A., 1986. Biochemical disposal of excess H⁺ in growing plants? *New Phytologist*, 104, pp.175–206.
- Ravet, K. et al., 2009. Ferritins control interaction between iron homeostasis and oxidative stress in *Arabidopsis*. *The Plant journal : for cell and molecular biology*, 57(3), pp.400–12.

- Ricoult, C. et al., 2006. Characterization of alanine aminotransferase (AlaAT) multigene family and hypoxic response in young seedlings of the model legume *Medicago truncatula*. *Journal of experimental botany*, 57(12), pp.3079–89.
- Rocha, M. et al., 2010. Analysis of alanine aminotransferase in various organs of soybean (*Glycine max*) and in dependence of different nitrogen fertilisers during hypoxic stress. *Amino acids*, 39(4), pp.1043–53.
- Sambongi, Y., 1999. Mechanical Rotation of the c Subunit Oligomer in ATP Synthase (F₀F₁): Direct Observation. *Science*, 286(5445), pp.1722–1724.
- Sanchez, D.H. et al., 2008. Integrative functional genomics of salt acclimatization in the model legume *Lotus japonicus*. *The Plant journal : for cell and molecular biology*, 53(6), pp.973–87.
- Sánchez-Aguayo, I. et al., 2004. Salt stress enhances xylem development and expression of S-adenosyl-L-methionine synthase in lignifying tissues of tomato plants. *Planta*, 220(2), pp.278–85.
- Sanchez-Aguayo, I., Gonzalez-Utor, a L. & Medina, a, 1991. Cytochemical Localization of ATPase Activity in Salt-Treated and Salt-Free Grown *Lycopersicon esculentum* Roots. *Plant physiology*, 96(1), pp.153–8.
- Sato, S., Isobe, S. & Tabata, S., 2010. Structural analyses of the genomes in legumes. *Current opinion in plant biology*, 13(2), pp.146–52.
- Scholander, P. F., Bradstreet, E. D., Hemmingsen, E. A., H.H.T., 1965. Sap pressure in vascular plants - negative hydrostatic pressure can be measured in plants. *Science*, 148(3668), pp.339–346.
- Sekmen, A.H., Türkan, I. & Takio, S., 2007. Differential responses of antioxidative enzymes and lipid peroxidation to salt stress in salt-tolerant *Plantago maritima* and salt-sensitive *Plantago media*. *Physiologia plantarum*, 131(3), pp.399–411.
- Seo, J. & Lee, K.-J., 2004. Post-translational modifications and their biological functions: proteomic analysis and systematic approaches. *Journal of biochemistry and molecular biology*, 37(1), pp.35–44.
- Shalata, A. & Tal, M., 1998. The effect of salt stress on lipid peroxidation and antioxidants in the leaf of the cultivated tomato and its wild salt-tolerant relative *Lycopersicon pennelli*. *Physiologia Plantarum*, 104, pp.169–174.
- Smirnov, N., 1998. Plant resistance to environmental stress Nicholas Smirnov. *Current Opinion in Biotechnology*, (9), pp.214–219.
- Staudinger, C. et al., 2012. Possible Role of Nutritional Priming for Early Salt and Drought Stress Responses in *Medicago truncatula*. *Frontiers in plant science*, 3(December), p.18.

- Staudinger, C.E., 2010. Nitrogen-source related effects on drought stress response in *Medicago truncatula*.
- Stevens, P.F., 2001. Angiosperm Phylogeny. *Version 12*. Available at: <http://www.mobot.org> [Accessed October 3, 2012].
- Tardieu, F. et al., 1992. Xylem ABA controls the stomatal conductance of field-grown maize subjected to soil compaction or soil drying. *Plant, Cell and Environment*, 15(2), pp.193–197.
- Tardieu, François, 2012. Any trait or trait-related allele can confer drought tolerance: just design the right drought scenario. *Journal of experimental botany*, 63(1), pp.25–31.
- Terpolilli, J.J. et al., 2008. The model legume *Medicago truncatula* A17 is poorly matched for N₂ fixation with the sequenced microsymbiont *Sinorhizobium meliloti* 1021. *The New phytologist*, 179(1), pp.62–6.
- Thimm, O. et al., 2004. Mapman: a User-Driven Tool To Display Genomics Data Sets Onto Diagrams of Metabolic Pathways and Other Biological Processes. *The Plant Journal*, 37(6), pp.914–939.
- Trieu, a T. et al., 2000. Transformation of *Medicago truncatula* via infiltration of seedlings or flowering plants with *Agrobacterium*. *The Plant journal : for cell and molecular biology*, 22(6), pp.531–41.
- Tsiantis, M.S., Bartholomew, D.M. & Smith, J. a, 1996. Salt regulation of transcript levels for the c subunit of a leaf vacuolar H⁽⁺⁾-ATPase in the halophyte *Mesembryanthemum crystallinum*. *The Plant journal : for cell and molecular biology*, 9(5), pp.729–36.
- Türkan, İ. et al., 2005. Differential responses of lipid peroxidation and antioxidants in the leaves of drought-tolerant *P. acutifolius* Gray and drought-sensitive *P. vulgaris* L. subjected to polyethylene glycol mediated water stress. *Plant Science*, 168(1), pp.223–231.
- Uchida, A. et al., 2002. Effects of hydrogen peroxide and nitric oxide on both salt and heat stress tolerance in rice. *Plant Science*, 163(3), pp.515–523.
- Wallsgrave, R.M. et al., 1987. Barley mutants lacking chloroplast glutamine synthetase-biochemical and genetic analysis. *Plant physiology*, 83(1), pp.155–8.
- Wang, B.S., Ratajczak, Rafael & Zhang, J.H., 2000. Activity, amount and subunit composition of vacuolar-type H⁺-ATPase and H⁺-PPase in wheat roots under severe NaCl stress. *Journal of Plant Physiology*, 157(1), pp.109–116.
- Wang, C., Li, J. & Yuan, Ming, 2007. Salt tolerance requires cortical microtubule reorganization in *Arabidopsis*. *Plant & cell physiology*, 48(11), pp.1534–47.

- Wang, S. et al., 2011. Salt stress-induced disassembly of Arabidopsis cortical microtubule arrays involves 26S proteasome-dependent degradation of SPIRAL1. *The Plant cell*, 23(9), pp.3412–27.
- Wang, W.-B. et al., 2009. Analysis of antioxidant enzyme activity during germination of alfalfa under salt and drought stresses. *Plant physiology and biochemistry*, 47(7), pp.570–7.
- Wang, X., 2002. Phospholipase D in hormonal and stress signaling. *Current opinion in plant biology*, 5(5), pp.408–14.
- Weckwerth, W., 2011a. Green systems biology - From single genomes, proteomes and metabolomes to ecosystems research and biotechnology. *Journal of proteomics*, 75(1), pp.284–305.
- Weckwerth, W., 2011b. Unpredictability of metabolism--the key role of metabolomics science in combination with next-generation genome sequencing. *Analytical and bioanalytical chemistry*, 400(7), pp.1967–78.
- Welinder, K.G. et al., 2002. Structural diversity and transcription of class III peroxidases from Arabidopsis thaliana. *European Journal of Biochemistry*, 269(24), pp.6063–6081.
- Wienkoop, S. et al., 2006. Stable isotope-free quantitative shotgun proteomics combined with sample pattern recognition for rapid diagnostics. *Journal of Separation Science*, 29(18), pp.2793–2801.
- Wyk, B.-E., 2005. Handbuch der Nahrungspflanzen, Stuttgart: Tien Wah Press.
- Young, Nevin D et al., 2011. The Medicago genome provides insight into the evolution of rhizobial symbioses. *Nature*, 480(7378), pp.520–4.
- Zancani, M. et al., 2004. Evidence for the presence of ferritin in plant mitochondria. *European journal of biochemistry*, 271(18), pp.3657–64.
- Zhang, J. & Kirkham, M., 2006. Antioxidant responses to drought in sunflower and sorghum seedlings. *New Phytologist*, 132, pp.361–373.
- Zhang, Q. et al., 2012. Phosphatidic Acid Regulates Microtubule Organization by Interacting with MAP65-1 in Response to Salt Stress in Arabidopsis. *The Plant Cell*, pp.4555–4576.

8. Acknowledgement

My gratitude shall not be expressed to people rather than to the inspiring moments they shared with me. Those moments I will here picture and you are welcome to find yourself in the following lines.

Thanks to many, I grew up with an open mind, a good heart and the persistent urge to explore whatever mentally or earthly thing there was on my way. The last year of my work my interest grew steadily and I was well taken care of and learned how to stay secure in the laboratory. I was taught a clean and precise working style which I sometimes failed to follow due to amusing chats. Enjoyable conversations did go on in the climatic chamber between snipping leaves and roots, weighing and measuring bombastic potentials. Those were motivating moments which gave me power for data processing of which I despaired anyway. My cries for help were often heard and by relaxing coffee breaks I regained inner balance. If it was profession I was seeking to make me understand or feedback me, I could always find expertise next door. Above all, at every day during this time, there was someone who I could tell my daily stories to and laugh together whether those were sad or funny.

A. Attachments

A.1. Supplemental nutrient solutions EC-values

Table 8.1: Electrical conductivity of nutrient solutions

nutrient solution	EC $\mu\text{S}/\text{cm}$
2.5 mM NH_4NO_3	38
2.5 mM NH_4NO_3 + 200 mM NaCl	436
no nitrogen	19
no nitrogen + 200 mM NaCl	419

A.2. Formulations

Table 8.2: TY-medium *S. meliloti*

chemical	quantity [g]
Peptone/Tryptone	8
Yeast extract	1
NaCl	2.8
Glucose	0.5
Agar agar Kobe 1	4
qs ddH ₂ O to 500ml	

Table 8.3: Cultivation medium *S. meliloti*

chemical	quantity [g]
K_2HPO_4	0.5
$\text{MgSO}_4 \cdot 7\text{H}_2\text{O}$	0.2
NaCl	0.1
Mannitol	10
Yeast extract	0.4
qs ddH ₂ O to 1000ml	

A.3. Significant changing root proteins

Table 8.4: Salt stress responding root proteins with alteration values in percentage; control values are 100%, significant p-values (<0.05) are provided in brackets. Rhizobia related proteins were not detected (nd) in fertilized plants and therefore not assigned (na) in control plants

root protein		stress alteration in %		control
accession	description	N-fix	N-fed	N-fix/N-fed
<i>photosystem</i>				
G8A279	Fructose-bisphosphate aldolase (Fragment)	ns	ns	212.6 (0.022)
<i>major CHO metabolism</i>				
G7KM93	Phosphorylase	18.8 (0.003)	ns	ns
G7JXA7	Alpha-D-xylosidase	ns	ns	11.3 (0)
<i>TCA cycle</i>				
B7FJJ4	Pyruvate dehydrogenase E1 component subunit beta	313.5 (0)	ns	ns
B7FM31	Pyruvate kinase (Fragment)	16.5 (0)	ns	ns
G7ITZ5	Aconitate hydratase	ns	47 (0.047)	ns
B7FGY5	Cytochrome b-c1 complex subunit	17.2 (0.001)	ns	ns
G7I9N0	ATP synthase subunit d	630.9 (0)	ns	ns
Q02735	Phosphoenolpyruvate carboxylase	ns	ns	313.4 (0.024)
G7IH71	Phosphoenolpyruvate-carboxylase	ns	ns	313.4 (0.024)
G7J5G7	Carbonic anhydrase	ns	ns	698.6 (0)
G7J5G9	Carbonic anhydrase	ns	ns	452.6 (0)
<i>mitochondrial electron transport</i>				
G7KSG6	Cytochrome c	ns	ns	41.4 (0)
G7K7W9	Cytochrome c	ns	ns	33.6 (0.001)
A2Q5X9	Cytochrome c, monohaem	ns	ns	36.7 (0)
Q92LK8	ATP synthase subunit beta	ns	ns	1372.9 (0)
<i>cell wall</i>				
G7L571	UDP-glucose 6-dehydrogenase	32.3 (0)	45.9 (0.007)	ns
G7JWW6	Alpha-1 4-glucan-protein synthase	22.3 (0.003)	ns	ns
<i>lipid metabolism</i>				
G7I9C1	Pyruvate kinase	16 (0)	ns	ns
Q1SN32	Pyruvate kinase	12.9 (0)	ns	ns
Q2HUA3	Phospholipase D	17.6 (0)	40.6 (0.026)	ns
G7K6T1	Acyl-CoA-binding protein	ns	ns	48.2 (0.003)
<i>N-metabolism</i>				
O04998	Glutamine synthetase	ns	ns	293.6 (0)
B7FJE6	Glutamine synthetase (Fragment)	ns	ns	353.7 (0.024)
<i>amino acid metabolism</i>				
G7JCK0	Ketol-acid reductoisomerase	ns	ns	711.4 (0)
Q40328	Asparagine synthetase	362 (0.009)	ns	ns
O24483	Asparagine synthetase	408 (0.007)	ns	ns
Q40325	Aspartate aminotransferase	ns	ns	1339 (0)
G7K3M9	Cysteine synthase	ns	ns	1473.7 (0)

<i>metal handling</i>				
Q9ZP90	Ferritin	ns	ns	25.6 (0.049)
G7JLS7	Ferritin	ns	ns	272.9 (0.007)
G7IBL7	Albumin-2	ns	ns	14.4 (0)
Q8H1L8	Manganese superoxide dismutase (Fragment)	ns	218.1 (0.015)	ns
Q6J9X6	S-adenosylmethionine synthase (Fragment)	33.7 (0.016)	244.8 (0.034)	249.1 (0.024)
G7JK45	Monocopper oxidase-like protein SKU5	ns	ns	16.1 (0.005)
Q9SBR9	Basic blue protein	ns	ns	2239.1 (0)
<i>secondary metabolism</i>				
G7KER9	Hydroxymethylglutaryl-CoA synthase	ns	42 (0.049)	ns
G7KER8	Hydroxymethylglutaryl-CoA synthase	ns	30.8 (0.049)	ns
G7IEZ6	Chalcone-flavonone isomerase	ns	ns	47.2 (0)
G7K4Y9	Chalcone reductase	ns	ns	18.5 (0)
G7K4Z0	Chalcone reductase	ns	ns	16.7 (0)
G7J9I2	NAD(P)H-dependent 6'-deoxychalcone synthase	ns	ns	9.2 (0)
<i>hormone metabolism</i>				
G7LIY2	Lipoxygenase	333.1 (0.002)	ns	ns
G7LIY9	Lipoxygenase	ns	ns	14.2 (0)
<i>stress abiotic</i>				
G7IMY4	Pathogenesis-related protein PR10	ns	ns	46.6 (0.006)
G7INB7	ABA-responsive protein ABR17	ns	ns	40.9 (0.004)
G7JGC6	Low-temperature inducible	ns	ns	2.2 (0)
G7LFU4	MLP-like protein	ns	ns	9.8 (0)
<i>redox</i>				
Q45NL7	Thioredoxin	ns	306.4 (0.001)	ns
A1BLP6	Thioredoxin	ns	295.5 (0.001)	ns
<i>stress biotic</i>				
G7KG90	Stress-induced-phosphoprotein	442.1 (0)	ns	8 (0)
G7JJK5	Disease resistance response protein	ns	36.2 (0.017)	1.5 (0)
G7KMI6	Kunitz-type trypsin inhibitor-like 1 protein	ns	397.7 (0)	ns
<i>alcohol dehydrogenase</i>				
G7J5M7	Alcohol dehydrogenase	ns	ns	680.4 (0)
G7J5M6	Alcohol dehydrogenase	ns	ns	444.8 (0)
G7J5N1	Alcohol dehydrogenase	ns	ns	364.3 (0)
<i>peroxidase</i>				
G8A191	Peroxidase	ns	325.5 (0.003)	ns
G8A179	Peroxidase	ns	299.2 (0.003)	ns
G7JUC8	Peroxidase	ns	41.3 (0.01)	30 (0.009)
G7IJV0	Peroxidase	ns	ns	38.2 (0)
G7KX25	Peroxidase	ns	ns	37.7 (0.017)
G7KFM2	Peroxidase	ns	ns	24.9 (0)
<i>RNA-regulation</i>				
G7IMZ2	Disease resistance response protein Pi49	ns	32.3 (0.008)	14.4 (0.001)
G7JA80	Glycine-rich RNA-binding protein	ns	44.6 (0.007)	9.3 (0)
G7KC05	40S ribosomal protein S10-like protein	ns	ns	591.5 (0.049)
G7KC06	40S ribosomal protein S10-like protein	ns	ns	386.8 (0.049)

G7JJ57	RNA-binding protein	ns	ns	18.7 (0)
G7JHA8	Glycine-rich RNA binding protein	ns	ns	27 (0.001)
<i>protein regulation</i>				
G7JGQ4	Eukaryotic translation initiation factor 5A-1	ns	438.1 (0)	261.1 (0.005)
Q945F4	Eukaryotic translation initiation factor 5A-2	ns	523.2 (0)	311.8 (0.005)
B7FHA1	Proteasome subunit alpha type	ns	231.6 (0.001)	253.4 (0.001)
Q2HTA3	26S proteasome regulatory subunit-like protein	ns	222.2 (0.005)	ns
G7LB82	Proteasome subunit alpha type	27.9 (0)	ns	ns
B7FGZ8	Proteasome subunit beta type	219.6 (0.035)	ns	38.1 (0.004)
G7JC94	60S acidic ribosomal protein p0	ns	ns	36.8 (0.001)
G7IJ13	Proteasome subunit alpha type	ns	ns	26.8 (0)
G7IV48	26S protease regulatory subunit 6B	ns	ns	8.8 (0.049)
P26564	Eukaryotic translation initiation factor 5A-1	287.8 (0)	ns	ns
P38661	Probable protein disulfide-isomerase A6	40.2 (0.012)	ns	ns
<i>signalling</i>				
G7KVQ8	Polygalacturonase inhibitor protein	426.5 (0)	ns	ns
G7L3N5	Calmodulin	ns	596.2 (0)	ns
G7KP29	Calmodulin	ns	ns	36.5 (0.012)
G7J2R7	Calnexin-like protein	ns	ns	17.2 (0)
G7IMU5	GTP-binding protein SAR1A	ns	ns	23.6 (0)
<i>cell organization</i>				
G7KB73	Annexin	ns	245.3 (0.001)	0.5 (0)
G7IL85	Actin	ns	ns	234.7 (0.046)
G7L826	Actin depolymerizing factor-like protein	ns	ns	48.5 (0.016)
<i>transport</i>				
G7JUD3	Plasma membrane H ⁺ -ATPase	ns	27.4 (0.013)	ns
G7JUD2	Plasma membrane H ⁺ -ATPase	42.9 (0.015)	ns	ns
G7KW90	V-type proton ATPase subunit C	33 (0)	ns	ns
Q2HUJ7	V-ATPase subunit C	32.2 (0)	ns	ns
G7JB62	Aquaporin protein PIP11	315.3 (0)	ns	ns
O22339	Aquaporin-like transmembrane channel protein	446.3 (0)	ns	ns
B7FMK2	V-type proton ATPase subunit E1	ns	ns	27.7 (0)
G7J868	YSL transporter	ns	ns	16.5 (0)
<i>defense response</i>				
Q43560	Class-10 pathogenesis-related protein 1	40.8 (0.014)	ns	47.9 (0.008)
G7J032	Major pollen allergen Bet v 1-L	ns	ns	17.5 (0)
P93333	PR10-1 protein	ns	ns	46.6 (0.006)
<i>acidic phosphatase activity</i>				
G7LGQ3	Acid phosphatase	ns	ns	604.9 (0)
G7LGQ4	Stem 28 kDa glycoprotein	ns	ns	27.6 (0)
<i>others</i>				
G7JQL0	Glucan endo-1,3-beta-glucosidase	ns	ns	49.4 (0.012)
B7FIM0	Caffeic acid 3-O-methyltransferase	ns	217.6 (0.004)	ns
G7JXI1	Thiosulfate sulfurtransferase	2187.5 (0)	ns	ns

G8A207	Remorin	547.7 (0)	ns	18.5 (0)
Q9SBS0	O-diphenol-O-methyl transferase	ns	1269.9 (0)	ns
Q40314	Acidic glucanase	ns	39 (0.014)	ns
A9YYK4	Acidic glucanase	ns	34.1 (0.013)	ns
O24076	Guanine nucleotide-binding protein subunit beta-like protein	36.6 (0.001)	ns	295.4 (0)
Q40333	Chalcone reductase	ns	ns	25 (0)
G7IG38	Narbonin	ns	ns	21.6 (0.012)
G7ZXA1	Narbonin	ns	ns	4.8 (0)
G9JZL3	Putative nuclear acid binding protein	ns	ns	27.6 (0)
P28014	Translationally-controlled tumor protein homolog	ns	ns	46.5 (0.028)
<i>symbiotic interaction</i>				
G7KGT0	Leghemoglobin	ns	nd	na
G7K1Z7	Leghemoglobin	ns	nd	na
G7KGN2	Leghemoglobin	ns	nd	na
G7K1Z9	Leghemoglobin	ns	nd	na
P27992	Leghemoglobin 1	ns	nd	na
P27993	Leghemoglobin 2	ns	nd	na
Q8W0Y5	Enod8.1	ns	nd	na
O81262	Early nodule-specific protein	ns	nd	na
G7I8F0	Early nodulin	ns	nd	na
<i>Sinhorhizobium meliloti</i>				
Q92LJ5	Succinyl-CoA ligase [ADP-forming] subunit alpha	ns	nd	na
Q9EYG9	Succinyl-CoA ligase [ADP-forming] subunit beta	ns	nd	na
Q9XD74	Superoxide dismutase [Mn]	ns	nd	na
Q9R9N4	Pyruvate dehydrogenase E1 component subunit beta	ns	nd	na
Q92LK6	ATP synthase subunit alpha	ns	nd	na
Q92PL0	Putative ABC transporter ATP-binding protein	ns	nd	na
P09820	Protein fixC	ns	nd	na
Q92LJ6	Probable dihydrolipoamide succinyl transferase component of 2-oxoglutarate dehydrogenase complex (E2) protein	ns	nd	na
Q92NR8	Probable cold shock transcription regulator	ns	nd	na
Q92L56	Probable aconitate hydratase	ns	nd	na
Q92PY6	Peptidyl-prolyl cis-trans isomerase	ns	nd	na
Q92ZL4	Nitrogenase protein alpha chain	ns	nd	na
P00460	Nitrogenase iron protein	ns	nd	na
Q92ZL3	NifK nitrogenase molybdenum-iron protein beta chain	ns	nd	na
Q9EYJ6	Malate dehydrogenase	ns	nd	na
Q92ZN9	FixO2 cytochrome c oxidase subunit	ns	nd	na
Q925Y6	Elongation factor Tu	ns	nd	na
Q92QH2	Elongation factor G	289.7 (0.037)	nd	na

P02344	DNA-binding protein HRm	ns	nd	na
Q9R9N3	Dihydrolipoyllysine-residue acetyltransferase component of pyruvate dehydrogenase complex	ns	nd	na
O33915	Citrate synthase	ns	nd	na
P19372	Acyl carrier protein AcpP	ns	nd	na
Q92N68	50S ribosomal protein L25	ns	nd	na
P14129	30S ribosomal protein S1	ns	nd	na
P42374	Chaperone protein DnaK	ns	nd	na
Q92ZQ4	60 kDa chaperonin 4	ns	nd	na
P35469	60 kDa chaperonin 1	ns	nd	na
Q92ZQ3	10 kDa chaperonin 4	ns	nd	na
P35473	10 kDa chaperonin 1	ns	nd	na
Q92SW0	Polyribonucleotide nucleotidyltransferase	49 (0.021)	nd	na
Q9R9N5	Pyruvate dehydrogenase E1 component subunit alpha	33.4 (0)	nd	na
Q92Q96	Dihydrolipoyl dehydrogenase	14.3 (0)	nd	na
Q7APA7	Probable 2-oxoglutarate dehydrogenase E1 component protein	31.5 (0.004)	nd	na
<i>Sinhorhizobium medicae</i>				
A6UDP1	Succinyl-CoA ligase [ADP-forming] subunit alpha	ns	nd	na
A6U713	Superoxide dismutase	ns	nd	na
A6UDM3	ATP synthase subunit alpha	ns	nd	na
A6UME8	Nitrogenase protein alpha chain	ns	nd	na
A6U849	50S ribosomal protein L10	ns	nd	na
A6UF46	30S ribosomal protein S1	ns	nd	na
A6UMF3	FAD dependent oxidoreductase	22.6 (0)	nd	na
A6U8E8	Dehydrogenase E1 component	25.9 (0)	nd	na
A6U9I3	FeS assembly protein SufB	231.7 (0.032)	nd	na
A6U9N3	Isocitrate dehydrogenase [NADP]	264.4 (0.045)	nd	na
<i>"putative" uncharacterized proteins</i>				
Q92PL1	similar 100% F6E1F1, FeS assembly protein SufD, e=0	530.9 (0)	ns	ns
B7FGN7	similar 96.0% A2ICP9, Ran1, Pisum sativum (Garden pea), e=1.0×10 ⁻¹⁶³	361.5 (0.011)	ns	ns
B7FIV8	similar 86% G7IDU4, Protein disulfide-isomerase, Medicago truncatula (Barrel medic) (Medicago tribuloides), e=0	47.2 (0.012)	ns	ns
B7FJS1	similar 95.0% P42654, 14-3-3-like protein B, Vicia faba (Broad bean) (Faba vulgaris)	396.7 (0.001)	ns	ns
B7FMA6	similar 98.0% P26564, Eukaryotic translation initiation factor 5A-1, Medicago sativa (Alfalfa), e=1.0×10 ⁻¹¹¹	291.6 (0)	ns	ns
B7FMM0	similar 99.0% B7FMR1, Elongation factor 1-beta, Medicago truncatula (Barrel medic) (Medicago tribuloides), e=1.0×10 ⁻¹⁵⁴	734.8 (0)	ns	ns
B7FHJ3	similar 99.0% G7JB62, Aquaporin protein PIP11, Medicago truncatula (Barrel medic) (Medicago tribuloides)	877.7 (0)	ns	ns

B7FH69	similar 99.0% G7IFU0, Actin depolymerizing factor, <i>Medicago truncatula</i> (Barrel medic) (<i>Medicago tribuloides</i>), $e=2.0 \times 10^{-96}$	299.8 (0.004)	ns	ns
B7FN14	similar 99.0% G7J9M6, Ribosomal protein L9, <i>Medicago truncatula</i> (Barrel medic) (<i>Medicago tribuloides</i>), $e=1.0 \times 10^{-133}$	ns	12.5 (0)	ns
Q92PB9	similar 100% F7X7D1, Putative uncharacterized protein, <i>Sinorhizobium meliloti</i> (strain SM11), $e=1.0 \times 10^{-119}$	284.3 (0.002)	ns	ns
B7FM06	similar 84.0% G0T440, Purple acid phosphatases, <i>Glycine max</i> (Soybean) (<i>Glycine hispida</i>), $e=0$	330.8 (0)	ns	18 (0.002)
B7FGX0	similar 98.0% G7L8G2, MLP-like protein, <i>Medicago truncatula</i> (Barrel medic) (<i>Medicago tribuloides</i>), $e=1.0 \times 10^{-103}$	230.4 (0.018)	ns	32.1 (0.001)
B7FN11	similar 96.0% Q9FSZ5, GTP-binding protein, <i>Cicer arietinum</i> (Chickpea) (Garbanzo), $e=1.0 \times 10^{-161}$	289.6 (0.014)	ns	ns
B7FGV3	similar 98% Q9FSZ5, GTP-binding protein, <i>Cicer arietinum</i> (Chickpea) (Garbanzo), $e=1.0 \times 10^{-165}$	303.2 (0.013)	ns	ns
G7I4F8	similar 60.0% Q0JDA2, Os04g0418000 protein, <i>Oryza sativa</i> subsp. <i>japonica</i> (Rice), $e=2.0 \times 10^{-72}$	ns	ns	7.9 (0)
Q92RQ0	similar 72.0% E0MQA5, Inositol monophosphatase family protein, $e=1.0 \times 10^{-39}$	ns	ns	939.5 (0)
B7FGT6	similar 93.0% G7KC05, 40S ribosomal protein S10-like protein, protein S10-like protein <i>Medicago truncatula</i> (Barrel medic) (<i>Medicago tribuloides</i>), $e=1.0 \times 10^{-118}$	ns	ns	377.3 (0.049)
B7FJC8	similar 99.0% I1MDT4, Actin, <i>Medicago truncatula</i> (Barrel medic) (<i>Medicago tribuloides</i>), $e=0$	ns	ns	233.3 (0.046)
B7FKF4	similar 76.0% B9RKV9, Ankyrin repeat domain protein, putative, <i>Ricinus communis</i> (Castor bean), $e=0$	ns	ns	49.7 (0.005)
B7FGS4	similar 95.0% G8A189, 40S ribosomal protein S5, <i>Medicago truncatula</i> (Barrel medic) (<i>Medicago tribuloides</i>), $e=1.0 \times 10^{-130}$	ns	ns	34.5 (0.003)
B7FN36	similar 57.0% P22778, ATP synthase subunit O, mitochondrial, <i>Ipomoea batatas</i> (Sweet potato) (<i>Convolvulus batatas</i>), $e=2.0 \times 10^{-89}$	ns	ns	29.3 (0)
B7FMA7	similar 99.0% G7IMU5, GTP-binding protein SAR1A, <i>Medicago truncatula</i> (Barrel medic) (<i>Medicago tribuloides</i>), $e=1.0 \times 10^{-138}$	ns	ns	23.3 (0)
B7FIX8	similar 99.0% G7K4Z0, Chalcone reductase, <i>Medicago truncatula</i> (Barrel medic) (<i>Medicago tribuloides</i>), $e=0$	ns	ns	20 (0)
B7FHM1	similar 73.0% Q5I2D1, Caffeoyl CoA 3-O-methyltransferase, <i>Betula platyphylla</i> (Asian white birch), $e=1.0 \times 10^{-130}$	ns	ns	17.4 (0)
B7FI34	similar 99.0% G7J9I2, NAD(P)H-dependent 6'-deoxychalcone synthase, <i>Medicago truncatula</i> (Barrel medic) (<i>Medicago tribuloides</i>), $e=0$	ns	ns	2.5 (0)
B7FMQ5	similar 85.0% B9RCM6, Vacuolar ATP synthase subunit E, putative, <i>Ricinus communis</i> (Castor bean), $e=1.0 \times 10^{-126}$	ns	ns	17.7 (0)
B7FK08	similar 82.0% G5DWW8, GAMMA carbonic anhydrase, <i>Silene latifolia</i> (White campion) (Bladder campion), $e=1.0 \times 10^{-129}$	ns	ns	8.7 (0)

A.4. Significant changing shoot proteins

Table 8.5: Salt stress responding shoot proteins with alteration values in percentage. Control values are 100%. significant p-values (<0.05) are provided in brackets

shoot Protein		stress alteration in %		control
accession	description	N-fix	N-fed	N-fix/N-fed
<i>photosystem</i>				
G7K694	Fructose-bisphosphate aldolase	38.1 (0.015)	ns	ns
G7K4T4	Fructose-bisphosphate aldolase	ns	29.9 (0.001)	ns
G7JE46	Thylakoid lumenal 16.5 kDa protein	27.9 (0)	ns	ns
<i>minor CHO metabolism</i>				
G7LAD5	L-myo inositol-1 phosphate synthase	ns	396.3 (0.005)	ns
<i>glycolysis</i>				
G7KfV2	UTP-glucose 1 phosphate uridylyltransferase	298.2 (0.007)	ns	ns
<i>gluconeogenesis</i>				
G7JTZ0	Malate dehydrogenase	25.9 (0.023)	ns	ns
<i>mitochondrial electron transport</i>				
G7J108	ATP synthase subunit beta	9.1 (0)	ns	ns
G7I9Q9	ATP synthase subunit alpha	ns	329.5 (0.008)	ns
<i>lipid metabolism</i>				
G7JID0	Non-specific lipid-transfer protein	40.4 (0.049)	ns	ns
<i>amino acid metabolism</i>				
G7JYY7	Alanine aminotransferase	30.9 (0.025)	ns	ns
G7J014	Alanine glyoxylate aminotransferase	ns	286.7 (0.003)	ns
G7JJ96	Aminomethyltransferase	34.3 (0.048)	ns	ns
Q9XQ94	Glutamine synthetase leaf isozyme, chloroplastic	310.3 (0.009)	217.6 (0.038)	ns
<i>metal handling</i>				
G7JLS7	Ferritin	ns	337.3 (0.004)	272.9 (0.007)
G7K283	Ferritin	ns	211.5 (0.001)	ns
A5HKJ9	Ferritin	ns	1123.4 (0)	ns
<i>tetrapyrrole synthesis</i>				
G4W9I5	Glutamate 1-semialdehyde aminotransferase	ns	ns	442.8 (0.897)
<i>stress abiotic</i>				
G7KWU8	Heat shock protein	26.2 (0.046)	ns	ns
G7JGC9	Low-temperature inducible	ns	316.8 (0.001)	ns
Q1SKX2	Chaperone DnaK	28.9 (0.043)	ns	ns
<i>redox</i>				
G7IE32	2-Cys peroxiredoxin BAS1	ns	211.5 (0.047)	ns
G7J4Y2	Ascorbate peroxidase	ns	ns	479.4 (0.627)
<i>RNA-regulation</i>				
G7IED2	MRNA-binding protein	29.4 (0.007)	ns	ns
G7IED1	MRNA-binding protein	28.5 (0.007)	ns	ns
G7JG67	Glycine-rich RNA binding protein	47.1 (0.048)	ns	ns

<i>protein regulation</i>				
G7JB01	40S ribosomal protein SA	ns	ns	199.6 (0.579)
G7JPH8	Photosystem II stability/assembly factor HCF136	ns	ns	743.8 (0.485)
<i>signalling</i>				
B7FIY3	14-3-3 protein	25.8 (0.003)	ns	ns
<i>cell organization</i>				
G7IAN2	Tubulin beta chain	ns	404.5 (0)	ns
G7IML1	Tubulin beta chain	423.5 (0)	ns	ns
G7JRA0	Tubulin beta chain	ns	403.3 (0)	ns
<i>others</i>				
O81391	Chlorophyll a/b binding protein	ns	219.8 (0.006)	ns
<i>"putative" uncharacterized proteins</i>				
B7FI87	similar 81.0% D2WL74, DHAR class glutathione transferase DHAR2, Populus trichocarpa (Western balsam poplar) (Populus balsamifera subsp. trichocarpa), e=1.0×10-122	255 (0.008)	ns	ns
B7FHX0	similar 98.0% P29500, Tubulin beta-1 chain, Pisum sativum (Garden pea), e=0	ns	401.3 (0.009)	ns
B7FL88	similar 99.0% G7KXT9, Heat shock protein, Medicago truncatula (Barrel medic) (Medicago tribuloides), e=0	22.8 (0.043)	ns	ns
B7FM02	similar 95.0% Q2PEW7, Putative rubisco subunit binding-protein alpha subunit, Trifolium pratense (Red clover), e=0	26.7 (0.05)	ns	ns
B7FKL0	similar 98.0% G7L754, Notum-like protein, Medicago truncatula (Barrel medic) (Medicago tribuloides), e=0	ns	ns	342.5 (0.241)
B7FMZ0	similar 71.0% A9PCJ3, Predicted protein, Populus trichocarpa (Western balsam poplar) (Populus balsamifera subsp. trichocarpa), e=1.0×10-47	ns	ns	249.8 (0.38)
B7FIV2	similar 99.0% G7JTE4, Aldose reductase, Medicago truncatula (Barrel medic) (Medicago tribuloides), e=0	ns	ns	239.7 (0.446)
B7FHD0	similar 82.0% Q0PN10, Glutathione S-transferase, Caragana korshinskii, e=1.0×10-141	ns	ns	227.5 (0.241)
B7FMR8	similar 99.0% G7ITL8, Flavoprotein wrbA, Medicago truncatula (Barrel medic) (Medicago tribuloides), e=1.0×10-144	ns	ns	225.4 (0.241)

A.5. Significant changing shoot peptides

Table 8.6: Salt stress responding shoot peptides with alteration values in percentage; control values are 100%. Significant p-values (<0.05) are provided in brackets. Changes which could not be assessed in stressed plants as proteins were not detected in control plants were not assigned (“na”)

m/z	Protein accession	Description	N-fix	N-fed
906.47	G7LDP4	ADP,ATP carrier protein	ns	3 (0.046)
AA: GNFLVDFLMGGVSAAVSK				
954.00	G7JQA7; G7JFY8	Apocytochrome f	na (0.034)	ns
AA: KYSEITFPILSPDPATK				
525.63	G7JLS7;Q9ZP90; A5HKJ9	Ferritin	ns	na (0.038)
AA: DVLAVPIAHNVSLAR				
787.95	G7JLS7;Q9ZP90; A5HKJ9	Ferritin	ns	na (0.011)
AA: DVLAVPIAHNVSLAR				
729.33	G7JG19;G7L520; G7KLK5;A2Q5A2; P04991	Ribulose biphosphate carboxylase large chain	1117(0.048)	ns
AA: GGLDFTKDDENVNSQPFmR				

A.6. Curriculum vitae

Reinhard Josef Turetschek

Date of Birth 28th of November, 1985

Place of Birth Mistelbach

Education

2000 - 2005 Technologisches Gewerbemuseum, Austria, A – Level

2010 – 2011 Erasmus, The University of Manchester, Life Science

2006 - present University of Vienna, Diploma-study of teaching biology and geography

Employment

2005 - 2006 Civil Service, Caritas Mobiles Hospiz

2007 - 2012 Facultas, Bookshop of Life Science Literature

2007 - 2012 Auring, Guidance of Biological Excursions

2008 - present University of Vienna, Zentraler Informatik Dienst, Tutor

Publications

2012 Possible role of nutritional priming for early salt and drought stress responses in *Medicago truncatula*, C. Staudinger, V. Mehmeti, R. Turetschek, V. Egelhofer, S. Wienkoop, *Frontiers in Plant Science*, 3:285.

Conference presentation

2/2013 Vienna International Plant Association Conference
Poster: Nutritional priming studies of *Pisum sativum* cv. Sirius to *Rhizobium* and mycorrhiza inoculation